Loss of the Sec1/Munc18-family proteins VPS-33.2 and VPS-33.1 bypasses a block in endosome maturation in *Caenorhabditis elegans*

Jachen A. Solinger and Anne Spang
Growth and Development, Biozentrum, University of Basel, CH-4056 Basel, Switzerland

ABSTRACT **The end of the life of a transport vesicle requires a complex series of tethering, docking, and fusion events. Tethering complexes play a crucial role in the recognition of membrane entities and bringing them into close opposition, thereby coordinating and controlling cellular trafficking events. Here we provide a comprehensive RNA interference analysis of the CORVET and HOPS tethering complexes in metazoans. Knockdown of CORVET components promoted RAB-7 recruitment to subapical membranes, whereas in HOPS knockdowns, RAB-5 was found also on membrane structures close to the cell center, indicating the RAB conversion might be impaired in the absence of these tethering complexes. Unlike in yeast, metazoans have two VPS33 homologues, which are Sec1/Munc18 (SM)-family proteins involved in the regulation of membrane fusion. We assume that in wild type, each tethering complex contains a specific SM protein but that they may be able to substitute for each other in case of absence of the other. Of importance, knockdown of both SM proteins allowed bypass of the endosome maturation block in *sand-1* mutants. We propose a model in which the SM proteins in tethering complexes are required for coordinated flux of material through the endosomal system.**

Monitoring Editor
Patrick J. Brennwald
University of North Carolina

Received: Dec 2, 2013
Revised: Sep 19, 2014
Accepted: Sep 23, 2014

INTRODUCTION

Extracellular components and fluids, as well as membrane-bound factors, including lipids, are internalized through a process collectively termed endocytosis. Endosomal pathways play a central role in membrane traffic in all eukaryotic cells. Endocytic carriers generated at the plasma membrane will fuse to form early endosomes, which are the crossroad of many trafficking pathways. A large fraction of endocytosed material will be recycled back to the plasma membrane (Besterman and Low, 1983; Steinman *et al.*, 1983; Chen *et al.*, 2006). Another subset of cargoes will reach the trans-Golgi network (TGN). A third group is sent to degradation. Sorting and selective sequestration of proteins and lipids will eventually lead to the maturation of early to late endosomes (reviewed in Huotari and Helenius, 2011). A hallmark of this maturation process is Rab conversion, in which the Rab5 GTPase present on early endosomes is replaced by the late endosomal Rab7 GTPase (Rink *et al.*, 2005; Poteryaev *et al.*, 2010). This event is regulated by the SAND1/MON1-CCZ1 complex, which interacts with the homotypic fusion and vacuole protein sorting (HOPS) tethering complex (Kinchen and Ravichandran, 2010; Poteryaev *et al.*, 2010). Finally, the matured late endosomes will fuse with lysosomes to form an endolysosome (Wickner, 2010; Huotari and Helenius, 2011). Through degradation of its internal lipid and protein content, the endolysosome eventually matures into a lysosome.

Besides the HOPS complex, at least one other tethering complex acts in the endosomal pathway in yeast: the class C core vacuole/endosome tethering (CORVET) complex is supposed to tether incoming endocytic vesicles at early endosomes (Balderhaar *et al.*, 2013). During endosome maturation, the early endosomal tethering factor CORVET is replaced by the late endosomal/lysosomal HOPS complex (Nickerson *et al.*, 2009; Balderhaar and Ungermann, 2013; Solinger and Spang, 2013). The HOPS complex in yeast has been characterized extensively and can be considered as prototype for endolysosomal tethers (Nickerson *et al.*, 2009; Pryor and Luzio, 2009;

This article was published online ahead of print in MBoC in Press (http://www.molbiolcell.org/cgi/doi/10.1091/mbc.E13-12-0710) on October 1, 2014.

Address correspondence to: Anne Spang (anne.spang@unibas.ch).

Abbreviations used: BSA-TR, bovine serum albumin–Texas Red; CORVET, class C core vacuole/endosome tethering; GFP, green fluorescent protein; HOPS, homotypic fusion and vacuole protein sorting; SM protein, Sec1/Munc18-related protein; SNARE, soluble *N*-ethylmaleimide–sensitive factor attachment receptor; TGN, trans-Golgi network.

Supplemental Material can be found at:
http://www.molbiolcell.org/content/suppl/2014/09/29/mbc.E13-12-0710v1.DC1

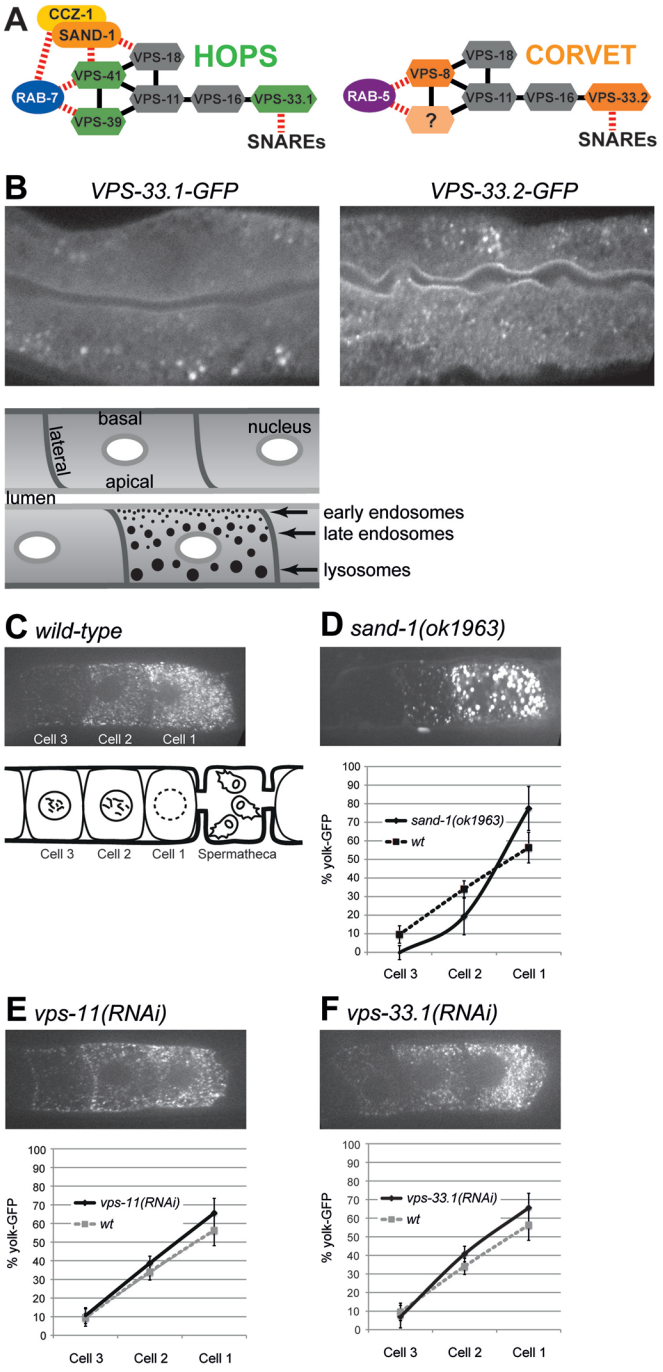

FIGURE 1: The HOPS complex is not involved in yolk granule biogenesis in oocytes. (A) Schematic depiction of HOPS complex with interactions between subunits with RAB-7, SAND-1/CCZ1, and SNAREs. CORVET complex is shown with described interactions between subunits, RAB-5, and SNAREs. (B) VPS-33.1 localizes to late endosomes/lysosomes, and VPS-33.2 localizes to early endosomes near the apical side of gut cells. Localization of VPS-33.2-GFP and VPS-33.1-GFP fusion proteins expressed from extrachromosomal arrays under their own promoter. (C–F) Yolk uptake is not affected by HOPS subunit knockdown. YP170-GFP content of three oocytes nearest to the spermatheca was analyzed (schematic view in C). Top, representative confocal microscopy pictures; bottom, quantification of 10 projected stacks ($N = 6$). A value of 100% corresponds to the average total yolk content of all three wild-type oocytes. (C) Yolk uptake in wild type is nearly linear. (D) *sand-1(ok1963)* deletion causes a delay in yolk uptake in cells 2 and 3 and yolk accumulation in cell 1. (E) Yolk uptake in *vps-11(RNAi)* worms is very similar to that in wild type (wild-type curve is shown in gray as a comparison). (F) *vps-33.1(RNAi)* oocytes show no defect in yolk uptake compared with wild type.

Wickner, 2010; Plemel *et al.*, 2011; Bröcker *et al.*, 2012). Both complexes share a common core, consisting of Vps11, Vps16, and Vps18 (Figure 1A). In addition, the tethering complexes have two distinct business ends. Two specific subunits are involved in the interaction with Rab GTPases, whereas a third subunit is a Sec1/Munc18-related (SM) protein and regulates soluble *N*-ethylmaleimide–sensitive factor attachment protein receptor (SNARE) complex assembly (Plemel *et al.*, 2011; Bröcker *et al.*, 2012; Graham *et al.*, 2013). Vps3 and Vps8 interact with Vps21 (yeast RAB-5), and Vps41 and Vps39 interact with Ypt7 (yeast RAB-7), whereas Vps33 binds the vacuolar quaternary SNARE complex (Lobingier and Merz, 2012; Figure 1A). Thus the tethers may also coordinate Rab GTPase function with SNARE assembly and membrane fusion. Therefore endosomal tethering complexes do more than just bring together two membrane-bound endocytic structures; they may play a central role in coordinating and controlling endosomal traffic (Solinger and Spang, 2013). In addition to the HOPS and CORVET complexes, some intermediates between CORVET and HOPS have been described, indicating that these complexes exist in a dynamic equilibrium (Peplowska *et al.*, 2007; Balderhaar *et al.*, 2013). Another complex, containing Vps45, plays a role in the biosynthetic pathway in yeast and possibly has more complex functions in metazoans, including the fusion of endocytic vesicles and recycling at early endosomes (Gengyo-Ando *et al.*, 2007; Morrison *et al.*, 2008; Furgason *et al.*, 2009; Rahajeng *et al.*, 2010). Only individual components of the HOPS complex have been studied in higher eukaryotes (Huizing *et al.*, 2001; Poupon *et al.*, 2003; Sriram *et al.*, 2003; Richardson *et al.*, 2004; Gissen *et al.*, 2005; Hermann *et al.*, 2005; Pulipparacharuvil *et al.*, 2005; Kinchen *et al.*, 2008; Xiao *et al.*, 2009; Abenza *et al.*, 2010), but CORVET and other complexes also should exist to ensure proper tethering in the increasingly complex pathways of higher eukaryotes.

In this study, we performed a comprehensive RNA interference (RNAi) analysis of all CORVET- and HOPS-like genes in *Caenorhabditis elegans*. We provide strong evidence for the existence of the CORVET complex in metazoans. Loss of CORVET function may cause premature endosome maturation, whereas reduced HOPS function conceivably causes a delay in the same process. HOPS is potentially required to efficiently displace RAB-5 from maturing endosomes. CORVET and HOPS each contains a specific SM protein, which may provide fusion specificity. Of importance, concomitant loss of both SM proteins VPS-33.1 and VPS-33.2 relieved the endosome maturation block of a *sand-1* mutant, highlighting an important role of these tethering complex in controlling the flux through the endosomal pathway.

RESULTS

The HOPS complex contains the SM protein VPS-33.1

To gain a better understanding of endosomal transport, we sought to analyze tethering complexes along the endocytic pathway and identified homologues of subunits of yeast HOPS and CORVET in worms, flies, and humans through database searches (Solinger and Spang, 2013). We found homologues for each of the subunits of the yeast HOPS and CORVET complexes, except for Vps3. Not unexpectedly, some of the HOPS/CORVET components had more than one homologue in metazoans. Because *C. elegans* contains two isoforms of the SM protein Vps33 (Table 1), we sought first to determine whether each tethering complex contained a specific SM protein.

			Wild-type worms			*sand-1(ok1963)* worms					
			Oocytes	Gut		Oocytes				Gut	
O: observed X: not observed		Synthetic interaction with *sand-1*	Yolk uptake defect	Enlarged endosomes with RAB-5 and RAB-7	Apical RAB-5 accumulation	Peripheral yolk granules	Central yolk granules	Enlarged yolk granules	Yolk granule size[a]	Apical RAB-5 accumulation	Dispersed RAB-7
Mock RNAi						O	X	O[b]	=[b]	X	O
Core	*vps-11*	O	X	X[c]	O	O	X	X[d]	<	O	O
	vps-16	O	X	X[c]	O	O	X	X[d]	<	O	O
	vps-18	O[e]	X	X[c]	O	O	X	X[d]	<	O	O
CORVET	*vps-8*	X	O	X[c]	O	O	X	X[d]	<	O	O
	vps-33.2	X	O	X[c]	O	O	X	O	>	X[f]	O
HOPS	*vps-39*	O	X	O	X	X	O	O	=	X	O
	vps-41	O	X	O	X	X	O	O	=	X	O
	vps-33.1	O	X	O	X	X	O	O	=	O	O
	vps-33.1+2	O	O	n.d.[g]	n.d.[g]	O	X	X[d]	<	X	X

[a]Granule size smaller than (<), equal to (=), or larger (>) than in *sand-1(ok1963)*.
[b]*sand-1(ok1963)* worms have enlarged yolk granules compared with wild type.
[c]Colocalization of RAB-5 and RAB-7 at the lumen.
[d]Vesicle size smaller than in *sand-1(ok1963)*.
[e]*vps-18(tm1125)* is synthetic lethal with *sand-1(ok1963)*.
[f]Vesicle size larger than in *sand-1(ok1963)*.
[g]Not determined.

TABLE 1: Summary of CORVET/HOPS phenotypes.

Because in yeast the CORVET complex is involved in fusion with the early endosome (Balderhaar *et al.*, 2013), we expected that in *C. elegans*, the knockdown of potential CORVET components would have a different phenotype than the *sand-1(ok1963)* deletion allele, which strongly delays maturation from early to late endosomes but has no defects in early endocytosis events (Poteryaev *et al.*, 2007, 2010). In contrast, a subset of HOPS complex members interact with SAND-1 (Poteryaev *et al.*, 2010), and hence their knockdown may enhance the *sand-1* phenotype because the transport down to the lysosome may be more severely blocked. To this end, we performed a genetic interaction analysis of all potential HOPS and CORVET components with *sand-1(ok1963)* using RNAi. The knockdown of components of the HOPS complex and potential CORVET-specific proteins was very efficient (Supplemental Figure S1A). Worms bearing a *sand-1(ok1963)* deletion allele show various defects at 20°C, including partial sterility (Poteryaev *et al.*, 2007). *vps-33.1(RNAi)* in a *sand-1(ok1963)* background caused a synthetic lethal phenotype, similar to the knockdown of the HOPS-specific subunits VPS-39 and VPS-41 and the core subunits VPS-11, VPS-16, and VPS-18 in the same background. In contrast, knockdown of neither the assumed CORVET component VPS-8 nor VPS-33.2 changed the *sand-1(ok1963)* phenotype in terms of viability (Table 1). Synthetic lethality was determined by the lack of viable offspring from the hermaphrodite that was subjected to double-stranded RNA treatment. Thus VPS-33.1 behaves similar to HOPS-specific subunits.

To extend these results, we determined the subcellular localization of both VPS-33 homologues by expressing green fluorescent protein (GFP) fusions under their own promoter in the intestine. Because the HOPS complex acts on late endosomes and lysosomes, we expected VPS-33.1 to be localized to those compartments. Indeed, VPS-33.1 localized mainly to lysosome-related gut granules and lysosomes and to a lesser extent to the apical surface of the intestinal epithelial cells (Figure 1B and Supplemental Figure S1B). In contrast, VPS-33.2::GFP lined the gut lumen and was also present in puncta, which might correspond to early endosomes (Figure 1B).

Finally, we determined the change in localization of the ESCRT-0 subunit HGRS-1 when either VPS-33.1 or VPS-33.2 level was reduced. HGRS-1 is present on endocytic structures (Roudier *et al.*, 2005), and according to its role in cargo sorting into intralumenal vesicles, HGRS-1 should be present on early and maturing endosomes. If VPS-33.1 is indeed a HOPS-specific component, HGRS-1 localization should be largely unaffected on early endosomes, but maturing endosomes might be altered by *vps-33.1(RNAi)*. In wild type, GFP::HGRS-1 was localized at the apical cortex and on endosomes (Supplemental Figure S1C). Knockdown of vps-33.1 left only the apical pool of HGRS-1 intact, which was somewhat reduced. These data suggest that VPS-33.1 represents the SM protein of the HOPS complex in *C. elegans*. It is noteworthy that *vps-33.2(RNAi)* caused an accumulation of GFP::HGRS-1 at the apical cortex, and distinct bright foci were detected, indicating that HGRS-1 was trapped on endosomes close to endocytosis sites.

Taking the subcellular localization and the genetic interactions together, our data are in support of VPS-33.1 being a component of HOPS and suggest that a CORVET complex exists also in *C. elegans*, which may contain VPS-33.2. Consistent with our data, *Drosophila* carnation, which is the closest homologue of VPS-33.1, is part of the HOPS complex (Akbar *et al.*, 2009).

The HOPS complex is not involved in yolk granule biogenesis in oocytes

To gain more direct insight into endocytic and endosomal functions of the HOPS complex in *C. elegans* oocytes, we used the well-established yolk-GFP system (Grant and Hirsh, 1999). The yolk protein YP170 is produced in intestinal cells, whence it is secreted into the body cavity. Maturing oocytes internalize yolk-GFP (YP170::GFP) through receptor-mediated endocytosis and transport it to yolk granules, which are supposed to be specialized lysosomes. YP170::GFP uptake can be readily detected in the most-proximal three oocytes near the spermatheca (Figure 1C). Yolk-GFP content of each cell was quantified and normalized to total yolk content in wild-type oocytes, yielding quantitative yolk uptake curves (Figure 1D). As previously reported, *sand-1(ok1963)* led to a mild defect in yolk uptake initially (Figure 1D, cells 2 and 3), which is compensated at later stages (cell 1; Poteryaev *et al.*, 2007). Of greater importance, the yolk granules were abnormally large. In contrast, no significant yolk uptake defects could be observed upon RNAi of HOPS and core subunits (Figure 1, E and F; Supplemental Figure S2, A and B). These data suggest that the HOPS complex is not essential for yolk uptake.

The HOPS complex acts on late endosomes and lysosomes in intestinal epithelial cells

Different cell types regulate transport distinctively to their needs. The great advantage of *C. elegans* is that we can assess transport readily in a variety of tissues in live animals (Solinger *et al.*, 2014). To this end, we generated a strain expressing integrated GFP::RAB-5 and mCherry::RAB-7 GTPases in intestinal epithelial cells (Chen *et al.*, 2006; Ackema *et al.*, 2013). This system allows the simultaneous observation of early endosomes associated with RAB-5 and of late endosomes/lysosomes bearing RAB-7 on their surface within the same cells (Figure 2, A–F). In wild-type worms, the RAB-5 compartment consists of small vesicles, which localize mostly in close proximity to the apical plasma membrane, which faces the gut lumen (Figures 1B and 2, A and G). Some small vesicles can also be observed throughout the cell and near the basolateral membrane (Figure 2A). The RAB-7 compartment consists of larger vesicles and sometimes interconnected structures that are not in direct contact with the plasma membrane and reside more centrally in the cell (Figure 2, B and G). The RAB-5 endosomes have no and the RAB-7 compartment only a slight overlap with autofluorescent gut granules, validating the use of this system (Supplemental Figure S2, D and E). In *sand-1(ok1963)* worms, the typical RAB-5–positive enlarged endosomal structures are apparent (Figure 2C), consistent with a defect in RAB conversion (Poteryaev *et al.*, 2010). Coherently, RAB-7 recruitment to membranes was impaired, and RAB-7 aggregates were observed (Figure 2D). The precise composition of these aggregates is unknown. Loss of the specific localization of both RAB-5 and RAB-7 compartments can be appreciated in profile plots across the gut (Figure 2G). This *sand-1* phenotype is similar to the one observed in coelomocytes (Poteryaev *et al.*, 2007). Knockdown of the HOPS-specific subunits *vps-33.1*, *vps-39*, and *vps-41* caused colocalization of large RAB-5– and RAB-7–positive vesicles on the basal side of the cells (Figure 2, E and F, and Supplemental Figure S2C). During the maturation process, endosomes are transported by motor proteins (Huotari and Helenius, 2011), and a notable fraction of lysosomes and lysosome-related organelles is localized close to the basal membrane in *C. elegans* intestinal cells (Nicot *et al.*, 2006; Ruaud *et al.*, 2009; Chotard *et al.*, 2010). Thus completion of Rab conversion may require the action of the HOPS complex in intestinal cells because RAB-5 cannot be efficiently displaced from endosomes. These data suggest two functions for the HOPS complex: one required for efficient displacement of RAB-5 from endosomes and hence at the same level as SAND-1, and a second one, downstream of SAND-1, since some RAB-7 was still recruited to

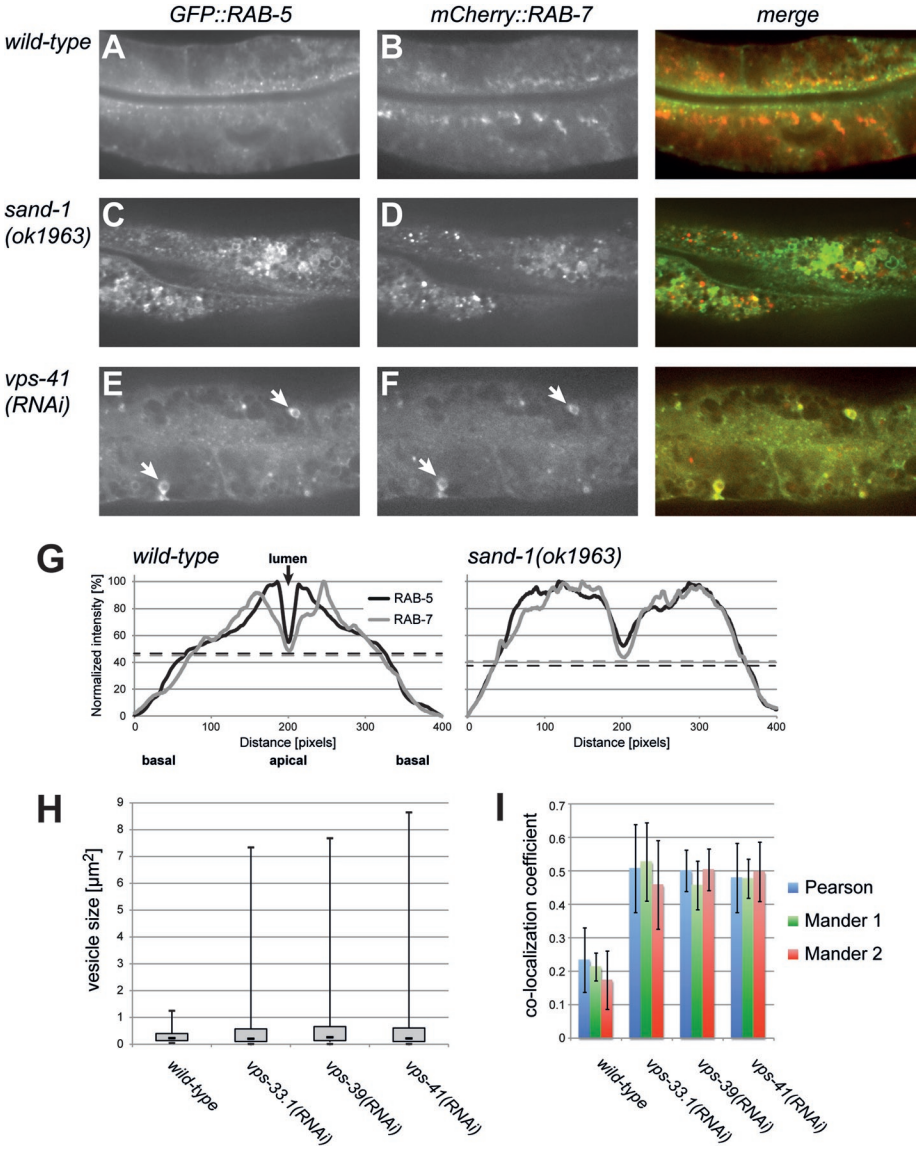

FIGURE 2: HOPS subunits have a role in late endosome/lysosome fusion. Analysis of GFP-RAB-5 and mCherry-RAB-7 simultaneously expressed in gut cells. (A) Wild-type worms with GFP-RAB-5 signal in small vesicles along the lumen and dispersed throughout the rest of the cell. (B) mCherry::RAB-7 signal in larger structures more centrally in the cell. (C) In *sand-1(ok1963)* gut cells, GFP::RAB-5 forms enlarged endosomes and aggregations of vesicles in large, grape-like structures. (D) mCherry::RAB-7 is dispersed and forms bright, dot-like aggregates. (E, F) *vps-41(RNAi)* causes formation of late endosomes/lysosomes with colocalization of GFP::RAB-5 and mCherry::RAB-7 signal in 60% of worms (indicated by arrows). (G) Profile plots across intestine. Brightness intensities were measured in a 200-pixel-wide stripe across gut pictures as shown in A–F. The length of the graphs is 400 pixels and corresponds to the width of the gut (indicated as distance on the *x*-axis; note that the gut lumen is centered at 200 pixels in these plots, apical membranes are directly adjacent to the lumen on both sides, and basal membranes are on the left and right). Curves from five worms were averaged and normalized to minimal (background outside the cell) and maximal values. The average background inside the cell is indicated by a hatched line and is similar to the value in the center of the graph, where the gut lumen lies. In wild type, GFP::RAB-5 signal is brightest near the apical membrane and decreases to the basal side, whereas mCherry::RAB-7 shows a peak more distant to the gut lumen. In *sand-1(ok1963)*, both signals are equally distributed across the gut cells, reflecting a loss of normal localization. (H) Vesicle size increase in knockdowns of HOPS-specific subunits *vps-33.1*, *vps-39*, and *vps-41*. Plots show 25th–75th percentile box, with median and whiskers indicating minimal and maximal values, respectively. Significantly larger RAB-5–positive vesicles are found in *vps-33.1(RNAi)* (p = 8.2E-15), *vps-39(RNAi)* (p = 8.2E-16), and *vps-41(RNAi)* (p = 5.9E-18) compared with wild-type (N = 6). (I) GFP-RAB-5 and mCherry-RAB-7 colocalize in HOPS-specific knockdown worms. Colocalization coefficients were measured in the gut (the region of interest was a 400-pixel square across the whole width of gut pictures as shown in A and E). Pearson and Mander coefficients were obtained using the JACoP plug-in of ImageJ after background subtraction (N = 5).

endosomes in the absence of HOPS complex components.

The HOPS complex acts downstream of the SAND-1–induced Rab conversion

To corroborate the foregoing findings, we decided to analyze the effects of RNAi of HOPS-specific subunits in a *sand-1(ok1963)* background. Loss of HOPS complex members slightly affected the uptake defects in *sand-1(ok1963)* (compare Figure 1D to Figure 3A and Supplemental Figure S3A), and yolk granules were often more clustered in a central position in cell 1. These data indicate a role for the HOPS complex in the transport or localization of endosomal structures and corroborate a function downstream of SAND-1.

HOPS and CORVET complexes are known to be involved in tethering of membranes and play a crucial role in subsequent membrane fusion (Stroupe *et al.*, 2006; Starai *et al.*, 2008; Balderhaar *et al.*, 2013). We reasoned that knocking down HOPS subunits should have an effect on the size of endosomes or yolk granules. Measurements of yolk granule size in *vps-16(RNAi)*, *vps-33.2(RNAi)*, *vps-8(RNAi)*, and *vps-33.1(RNAi)* worms showed no significant differences from wild type (Supplemental Figure S3B). This lack of an effect is potentially due to fast and efficient transport along the endocytic pathway. Because the maturation from early to late endosomes is strongly delayed in *sand-1* mutant animals, we checked yolk granule size in the sensitized *sand-1* background (Figure 3B). Knockdown of HOPS subunits had no effect on the yolk granule size in *sand-1(ok1963)* oocytes (Figure 3B). Finally, knockdown of the HOPS-specific subunits VPS-41 and VPS-39 did not change the *sand-1(ok1963)* phenotype in gut cells (Figure 3C and Supplemental Figure S3, C–F). We showed previously that SAND-1 physically interacts with components of the HOPS complex (Poteryaev *et al.*, 2010), similar to what was observed in yeast (Wang *et al.*, 2003; Solinger and Spang, 2013). Taken together, these data are consistent with a function of the HOPS complex downstream of SAND-1, but HOPS might in addition have a distinct function at the level of SAND-1.

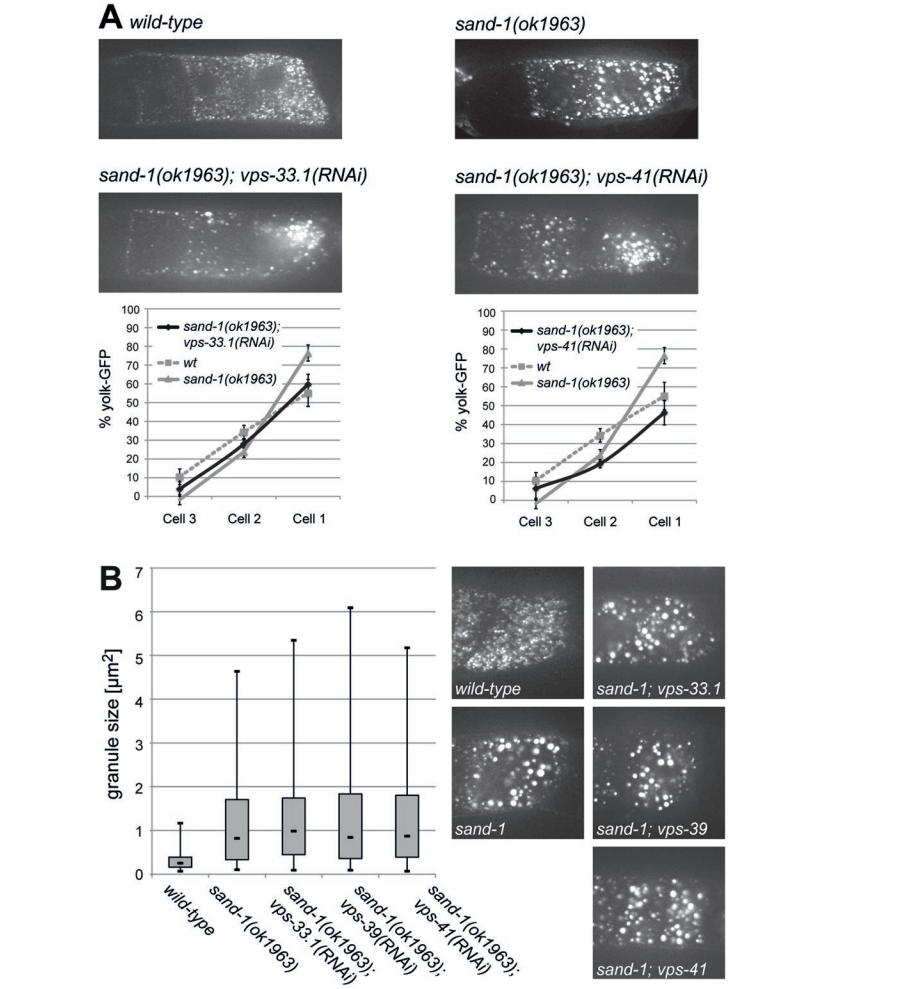

FIGURE 3: HOPS complex has a role together with SAND-1 and/or downstream of SAND-1 in late endosomes/lysosomes. (A) YP170-GFP uptake in *sand-1(ok1963); vps-33.1(RNAi)* and *sand-1(ok1963); vps-41(RNAi)* oocytes (for details see legend to Figure 1); wild-type and *sand-1(ok1963)* images are shown for comparison. (B) Yolk granule size in HOPS-subunit knockdown cells does not change in the *sand-1(ok1963)* background. Granule size was measured in cell 1 using particle analysis from ImageJ on a single plane from the *z*-stack. Right, representative images used for the measurements. Cells contained a minimum of ~40 vesicles each for large yolk granules (e.g., *sand-1(ok1963)*) and ~90 vesicles for small yolk granules (e.g., *wild type*). Box plots show median value in the center; each box represents 50% of all values (25% quartile to 75% quartile), and whiskers indicate minimal and maximal values, respectively ($N = 6$). Values for knockdowns are not significantly different from *sand-1* alone ($p = 0.16$ for *vps-33.1*, $p = 0.14$ for *vps-39*, and $p = 0.37$ for *vps-41*). (C) GFP-RAB-5 and mCherry-RAB-7 localization is unchanged in *sand-1(ok1963); vps-41(RNAi)* compared with *sand-1* alone (wild-type and *sand-1* gut pictures are shown for comparison).

The CORVET complex exists in *C. elegans* and affects early endosomal transport

The data presented so far would be consistent with a role of the HOPS complex in the late endocytic pathway, presumably at late endosomes and lysosomes, similar to what has been reported in yeast, *Drosophila*, and mammalian cells (Seals *et al.*, 2000; Akbar *et al.*, 2009; Swetha *et al.*, 2011; Pols *et al.*, 2013a). In addition, our initial analysis (Figure 1) hinted at the presence of CORVET in *C. elegans*. We wanted to corroborate these results and also test whether CORVET function would be conserved from yeast to metazoans. So far, CORVET has been studied only in yeast, where it is believed to promote fusion with early endosomes (Balderhaar *et al.*, 2013). We knocked down the CORVET-specific subunits VPS-8 and the SM protein VPS-33.2 (Figure 4A). Depletion of either subunit caused a slight yolk uptake defect in oocytes (Supplemental Figure S1D). Of greater importance, yolk-positive endocytic structures appeared to be tethered to large membranous organelles, which could represent enlarged endolysosomes. *vps-33.2(RNAi)* and *vps-8(RNAi)* resulted in a similar phenotype in oocytes, further suggesting that they might be indeed part of the same complex.

To extend these results, we analyzed the localization of RAB-5 and RAB-7 in intestinal cells upon knockdown of *vps-33.2* and *vps-8* (Figure 4B). In either case, GFP::RAB-5 was strongly enriched just underneath the apical plasma membrane when compared with wild type (Figures 4B and 2A). This finding is consistent with results suggesting a role of RAB-5 at clathrin-coated pits in *C. elegans* (Sato *et al.*, 2005). Thus initial uptake may only be slightly affected upon RNAi, but tethering and fusion of endocytic vesicles may be impaired. In contrast, the RAB-7–positive late endosomal compartment appeared largely unaffected by the knockdowns (Figures 4B and 2B). However, we noticed that a fraction of mCherry::RAB-7 was overlapping with the GFP::RAB-5 signal just underneath the apical plasma membrane, a localization we never observed in the wild-type background (Figures 4, B [arrowheads] and D, and 5C). An attractive explanation for this phenotype would be that RAB-7 was prematurely recruited onto

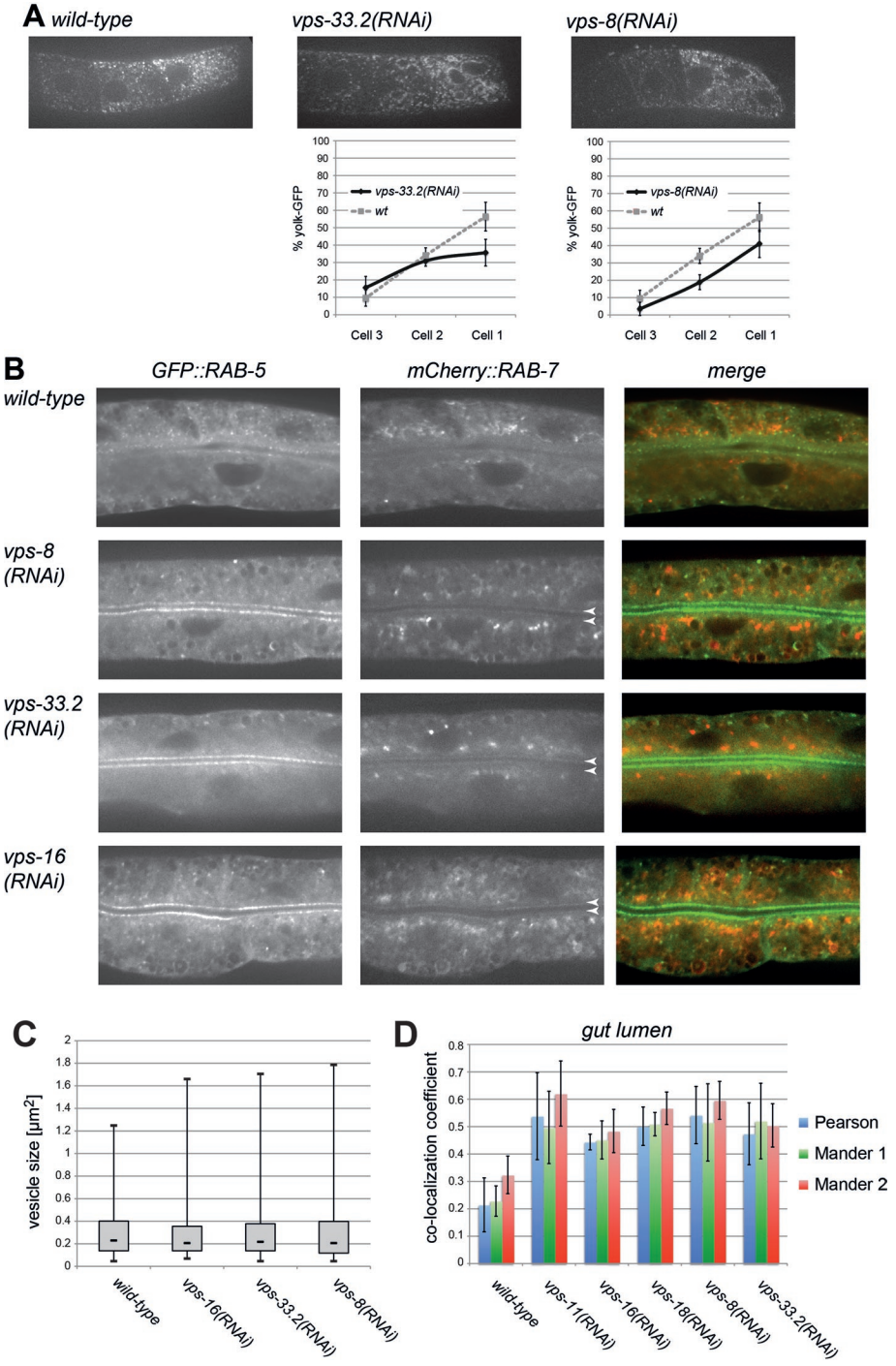

FIGURE 4: CORVET has an early role in endosome maturation. RNAi of CORVET subunits causes yolk uptake defects in oocytes and apical RAB-5 vesicle accumulation in gut cells. (A) YP170-GFP analyses in *vps-33.2(RNAi)* and *vps-8(RNAi)* oocytes (see legend to Figure 1 for details). Seventy percent of *vps-33.2(RNAi)* and *vps-8(RNAi)* worms show circular accumulations in cell 1. (B) *vps-8(RNAi)* causes GFP::RAB-5 vesicles to accumulate in two bright stripes along the lumen near the apical cell membrane (bright GFP-RAB-5 stripes in 85% of worms). RAB-7 vesicles are not affected by *vps-8(RNAi)*. *vps-33.2(RNAi)* (all worms analyzed) and *vps-11(RNAi)* (bright stripes in 90% of worms) cause a similar phenotype as *vps-8(RNAi)*. (C) The size of RAB-5–positive vesicles is unchanged in CORVET-subunit knockdowns. Box plots as in Figure 2H show no significant difference between *vps-16(RNAi)* ($p = 0.31$), *vps-33.2(RNAi)* ($p = 0.78$), *vps-8(RNAi)* ($p = 0.58$), and wild type ($N = 6$). (D) Colocalization of RAB-5 and RAB-7 at the gut lumen of CORVET and core subunit knockdown worms. Pearson and Mander coefficients were measured as in Figure 2I using a region of interest encompassing only a 30-pixel-wide (and 350-pixel-long) stripe directly at the gut apical membrane ($N = 5$).

endocytic structures under these conditions. Alternatively, movement of maturing endosomes from the apical surface could be affected.

The core components of the HOPS and CORVET complexes are shared in yeast (Ostrowicz *et al.*, 2010). Therefore we would expect that the knockdown of the core components results in a similar phenotype to that of CORVET-specific subunits because in yeast, CORVET acts upstream of HOPS. RNAi of the core components *vps-11*, *vps-16*, and *vps-18* also caused concentration of RAB-5 and RAB-7 at the apical membrane (Figure 4, B and D), whereas the RAB-7–positive late endosomal compartment remained unaffected (Figure 4B and Supplemental Figure S4, A and B). This accumulation at the apical cortex was specific, as there was no significant overlap of the RAB-5 and RAB-7 signals elsewhere in the cell (Supplemental Figure S4B). Our data are consistent with the existence of the CORVET complex in *C. elegans* and its functioning upstream of the HOPS complex. Thus our data point toward a conserved role from yeast to metazoans of the two tethering complexes. As in yeast, VPS-8 would be part of the CORVET complex, and VPS-33.2 would be a good candidate to fulfill the SM function of the complex. Furthermore our results may suggest that the CORVET complex plays a role in preventing premature Rab conversion.

The CORVET complex acts upstream of SAND-1

In yeast, CORVET interacts with Rab5 (Vps21) to promote fusion of Rab5-positive membranes (Balderhaar *et al.*, 2013), which would be a process upstream of Rab conversion. Therefore we asked whether CORVET would act also upstream of SAND-1 in *C. elegans*. The uptake defect of yolk protein into oocytes was stronger when either core components or the CORVET-specific subunits were down-regulated in *sand-1(ok1963)* compared with wild type (Figure 5A and Supplemental Figure S5A; compare to Figure 3, A and B, and Supplemental Figure S3A; summarized in Supplemental Figure S3G). Unlike in the wild-type background, yolk protein–positive structures did not cluster centrally but remained close to the plasma membrane. This localization of yolk granules near the cell periphery is indicative of a role of CORVET upstream of SAND-1.

To substantiate these results, we again checked the GFP::RAB-5 and mCherry::RAB-7 localization in *sand-1(ok1963)* gut cells. Loss of the CORVET-specific VPS-8 or the core components prevented the formation of

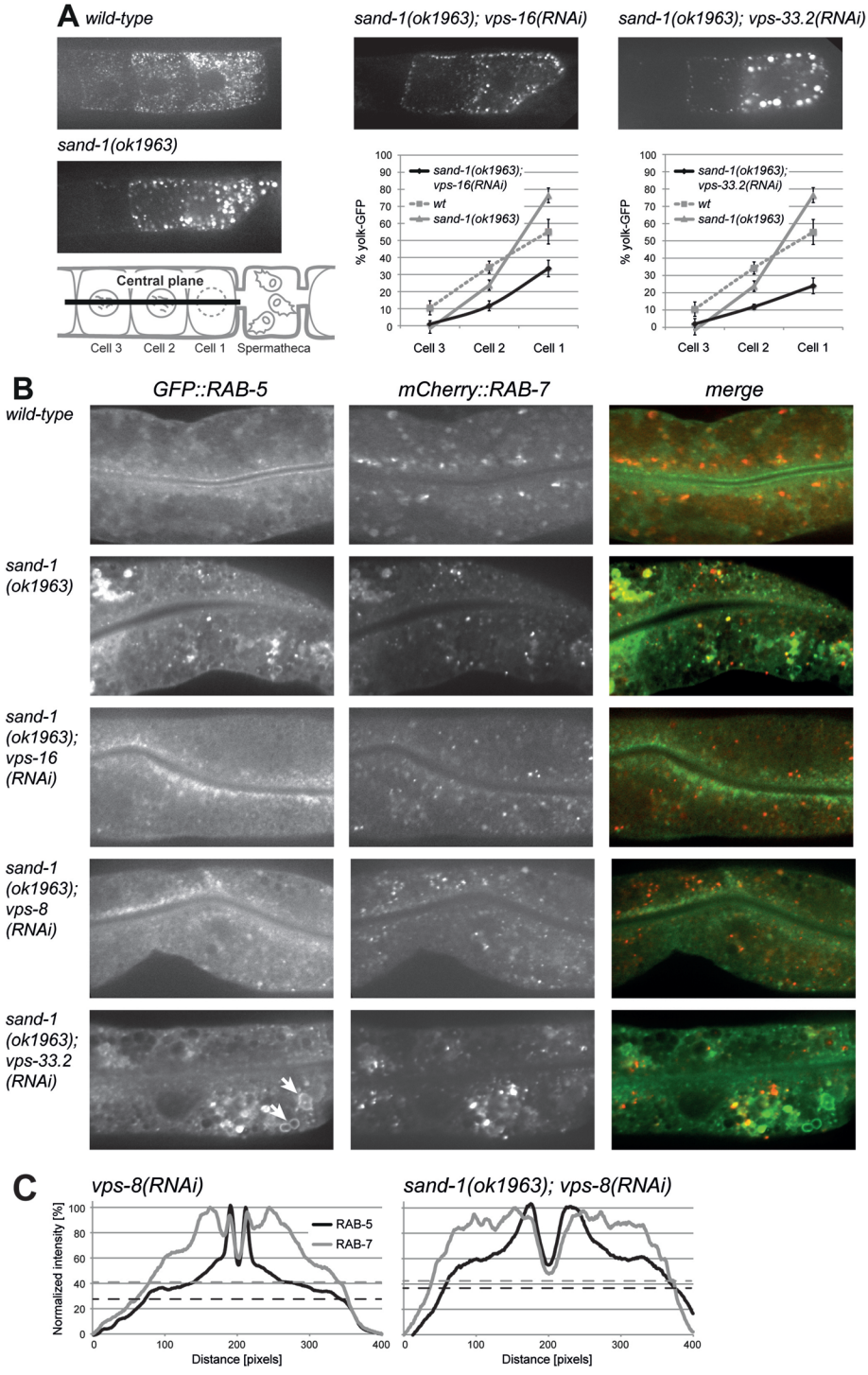

FIGURE 5: CORVET and core subunits have functions on early endosomes. (A) CORVET- subunit RNAi leads to peripheral yolk granule accumulation in a *sand-1(ok1963)* background. *sand-1(ok1963); vps-16(RNAi)* worms show YP170-GFP granules at cell periphery and yolk uptake defects. *sand-1(ok1963); vps-33.2(RNAi)* oocytes show a similar yolk uptake defect and localization of yolk granules at cell periphery as in *vps-16(RNAi)*. Wild-type and *sand-1* oocytes are shown for comparison. Schematic representation shows the central plane of pictures used to visualize peripheral yolk granules. (B) CORVET and core subunits function upstream of *sand-1* in the intestine. *sand-1(ok1963); vps-16(RNAi)* worms show accumulation of GFP::RAB-5 signal near the lumen at the apical side of cells (all worms analyzed). *sand-1(ok1963); vps-16(RNAi)* worms have a disorganized and dispersed mCherry::RAB-7 compartment, similar to *sand-1(ok1963)* alone, indicating an upstream function of *vps-16*. *sand-1(ok1963); vps-8(RNAi)* (in 80% of worms) look similar to *sand-1(ok1963)* worms. *sand-1(ok1963); vps-33.2(RNAi)* worms contain extra large RAB-5 compartments (indicated by arrows, quantification in Figure 6C). (C) Profile plots across *vps-8(RNAi)* guts (see legend to Figure 2G for description). Accumulation of GFP::RAB-5 near apical membrane results in two sharp peaks on both sides of the lumen. These peaks also appear in mCherry::RAB-7 curves, in addition to the normal localization more centrally in the cell (compare to wild-type RAB-7 graph in Figure 2G). In the *sand-1* background, the GFP::RAB-5 peaks move away from the apical membrane, and mCherry::RAB-7 is mislocalized (similar to the situation in *sand-1* alone in Figure 2G).

enlarged endosomes in *sand-1(ok1963)* intestinal cells (Figure 5, B and C, and Supplemental Figure S5B), whereas RAB-7 was still not recruited to endosomes (Supplemental Figure S6C). These data support CORVET acting upstream of SAND-1 along the endocytosis pathway.

vps-33.2(RNAi) causes the accumulation of "supersize" endosomes in *sand-1(ok1963)*

In contrast to the other CORVET or core components, loss of the SM subunit VPS-33.2 appeared to cause large endosomes in *sand-1(ok1963)* oocytes and intestinal cells (Figures 5, A and B, and 6, A–C, and Supplemental Figure S6, A and B). *sand-1* mutants already accumulate large endosomes in oocytes and gut epithelium (Poteryaev *et al.*, 2007; Figures 1D and 5A). To get a better measure of these phenotypes, we measured the size of the yolk-positive structures in the periphery of oocytes (Figure 6, A and B). Consistent with a role of the CORVET upstream of SAND-1 function, the size of yolk-positive structures was reduced when either the core components or the RAB-5 interacting subunit VPS-8 were silenced. *vps-33.2(RNAi)* in *sand-1(ok1963)* produced even bigger yolk-positive granules than *sand-1(ok1963)* itself (Figure 6B). Similarly, the RAB-5 positive endosomes in *sand-1(ok1963) vps-33.2(RNAi)* intestinal cells were larger than *sand-1(ok1963)* endosomes (Figure 6C and Supplemental Figure S6, A and B). Furthermore, these "supersize" endosomes often had an irregular shape, as if they were stalled during the fusion process (Figures 5B and 6C), sometimes with membranes still visible between the different entities. These results would be consistent with a delay of membrane fusion or fusion pore opening, as suggested for the yeast Vps33 (Pieren *et al.*, 2010). A possible explanation for the observed phenotype might be that one SM protein can substitute for the other in its absence. Hence, under these conditions, VPS-33.1 may be incorporated into

the CORVET and regulate the fusion process. The SM protein–interacting subunits are shared between HOPS and CORVET. In yeast, HOPS and CORVET exist in a dynamic equilibrium in which the RAB-interacting subunits can exchange and hence convert a HOPS complex into a CORVET complex and vice versa (Peplowska *et al*., 2007). Whereas there is only one Vps33 in yeast, *C. elegans* has VPS-33.1 and VPS-33.2. Thus we envisage the existence of complexes that have CORVET-specific RAB-5 interactors and a HOPS-specific SM protein and vice versa. The fusion process might be stalled because of the wrong SNARE-binding partners, therefore even enhancing the *sand-1(ok1963)* phenotype. This hypothesis seems plausible, given that *Drosophila* VPS33a (carnation) binds specifically to dsyntaxin16 (Golgi and lysosomes), whereas VSP33B binds to the early endosomal avalanche (dsyntaxin7; Akbar *et al*., 2009). These findings from *Drosophila* suggest that fusion specificity could be impaired also in *C. elegans*.

The analysis of the inverse experiment in which VPS-33.1 was missing in *sand-1(ok1963)* is complicated by the HOPS requirement to interact with RAB-7, which is not activated in *sand-1* mutants. Thus incorporation of VPS-33.2 into the HOPS complex would lead to a nonfunctional complex in the context of the *sand-1* mutant. We analyzed the phenotype of *sand-1(ok1963) vps-33.1(RNAi)* worms. Of interest, the phenotype in the gut, as judged by vesicle size, resembled more the knockdown of a core component or VPS-8 than other HOPS-specific components (Figure 6D and Supplemental Figures S3D and S6B). Given the dynamic equilibrium between HOPS and CORVET, VPS-33.2 concentration might become limiting, and the amount of functional CORVET complexes would be reduced. It is also conceivable that yet another protein could be recruited to the position of the SM protein in either tethering complex. Taken together, our data suggest that the SM protein in the tethering complexes is involved in the regulation of fusion of endocytic compartments.

Simultaneous loss of the SM proteins VPS-33.1 and VPS-33.2 bypasses the *sand-1(ok1963)* endocytosis block

The foregoing results suggest that both VPS-33 proteins could replace each other in the respective tethering complex in the absence of the bona fide subunit. Alternatively, the SM component position in the tethering complexes would remain vacant. The latter possibility suggests that simultaneous knockdown of both SM subunits would cause a strong delay in transport through the endosomal system and may have even additive effects. However, we observed quite the opposite effect, as concomitant knockdown of VPS-33.1 and VPS-33.2 in *sand-1(ok1963)* animals drastically reduced the size of the yolk-positive structures, approximating the size of wild-type yolk granules (Figure 7, A and B, and Table 2). Thus *vps-33.1+2(RNAi)* appears to at least partially rescue the large-early-endosome phenotype of *sand-1(ok1963)* worms. Moreover, the subcellular distribution of GFP::RAB-5– and mCherry::RAB-7–positive endosomes in *sand-1(ok1963) vps-33.1+2(RNAi)* was very similar to what we observed in wild-type intestinal cells (Figure 7C). RAB-7 was recruited to membranes again, presumably endosomes (Figure 7, C and D, Supplemental Figure S7, A and B, and Table 2). Similarly, the size of RAB-5–positive structures was reduced to almost wild-type levels (Figure 7E and Table 2). These results indicate both SM proteins may be involved in the regulation of the endocytic flux down to the lysosome. Moreover, they suggest that loss of both VPS-33 variants allows bypass of the *sand-1(ok1963)* block in endosome maturation. Although the endosome morphology was rescued, the *sand-1(ok1963) vps-33.1+2(RNAi)* worms still died, and loss of VPS-33.1+2 was synthetic lethal with *sand-1(ok1963)* (Table 1).

Cargo reaches the lysosomes in *sand-1(ok1963) vps-33.1+2(RNAi)* animals

If the transport through the endocytic pathway was restored in *sand-1(ok1963) vps-33.1+2(RNAi)*, cargo should reach the lysosomes efficiently under these conditions. To test this prediction, we turned to coelomocytes in *C. elegans*. Coelomocytes are scavenger cells in the body cavity and have been used to analyze transport from plasma membrane to lysosome (Fares and Greenwald, 2001a; Treusch *et al*., 2004; Poteryaev *et al*., 2007, 2010). Bovine serum albumin–Texas red (BSA-TR) is injected into the body cavity, and the coelomocytes internalize the dye and transport it to the lysosomes. Starting ~30 min after injection of BSA-TR, the dye accumulates in lysosomes (Poteryaev *et al*., 2007). In a *sand-1* mutant, the transport to lysosomes is strongly impaired, and even 60 min after injection, only a little BSA-TR reaches the lysosomes marked by LMP-1::GFP (Poteryaev *et al*., 2007; Figure 8A). This transport defect was not alleviated by the single knockdown of VPS-33.1 or VPS-33.2. However, similar to what we observed in intestinal cells, the BSA-TR–positive compartments were either smaller (*vps-33.1(RNAi)*) or larger (*vps-33.2(RNAi)*) than in *sand-1(ok1963)*. Of importance, knockdown of both VPS-33 proteins rescued the transport of BSA-TR to the lysosomes in the *sand-1* mutant, as after 30 min, almost all BSA-TR had reached the lysosome (Figure 8A). Thus loss of VPS-33.1+2 appears to bypass the block in the *sand-1* mutant.

The LMP-1::GFP–positive compartment in *sand-1(ok1963)* coelomocytes appeared to be affected by silencing either VPS-33 proteins but was restored in the *vps-33.1+2(RNAi)* (Figure 8A). Therefore we decided to analyze the LMP-1::GFP localization in intestinal cells. Most of the LMP-1::GFP was trapped in late endosome–like structures in *sand-1(ok1963)* animals (Figure 8B). As observed earlier, *vps-33.2(RNAi)* had a phenotype similar to *sand-1*, and *vps-33.1(RNAi)* caused entrapment of LMP-1::GFP in earlier compartments. The double knockdown partially rescued the transport block of *sand-1*, allowing LMP-1::GFP to move on to lysosomes (Figure 8B, arrows).

To corroborate these results, we expressed human transferrin receptor (hTfR) fused to GFP in the gut and analyzed its transport. This marker has been used to study endocytic traffic in *C. elegans* (Chen *et al*., 2006; Parker *et al*., 2009). It seems a reasonable assumption that part of the hTfR is degraded in lysosomes, and hence hTfR::GFP marks the entire endocytic pathway in gut cells (Supplemental Figure S7C). Our data presented so far are consistent with loss of VPS-33 SM proteins negatively influencing fusion specificity along the endosomal pathway. In support of this suggestion, hTfR-positive structures were dispersed throughout the cell in *vps-33.1+2(RNAi)* animals (Supplemental Figure S8).

In *sand-1(ok1963)* cells, hTfR was trapped in enlarged endosomes (Supplemental Figure S9). As observed earlier, *vps-33.2(RNAi)* had a *sand-1*-like phenotype, whereas *vps-33.1(RNAi)* confined the cargo in an earlier compartment. *vps-33-1+2(RNAi)* allowed a fraction of hTfR to proceed to lysosomal compartments (Supplemental Figure S8), alleviating the *sand-1(ok1963)* endosomal transport block.

Another way to check for restoration of transport to lysosomes in *sand-1(ok1963) vps-33.1+2(RNAi)* animals is via degradation of GFP in the lysosomes of coelomocytes. This assay measures at the same time the functionality of the lysosomes. Soluble secreted GFP is expressed in intestinal cells after heat shock, released into the body cavity, taken up by coelomcytes, and degraded in lysosomes (Fares and Greenwald, 2001b). In a *sand-1* mutant, this degradation is strongly delayed (Poteryaev *et al*., 2007). Combining *vps-33.1+2(RNAi)* with the *sand-1(ok1963)* mutation restored

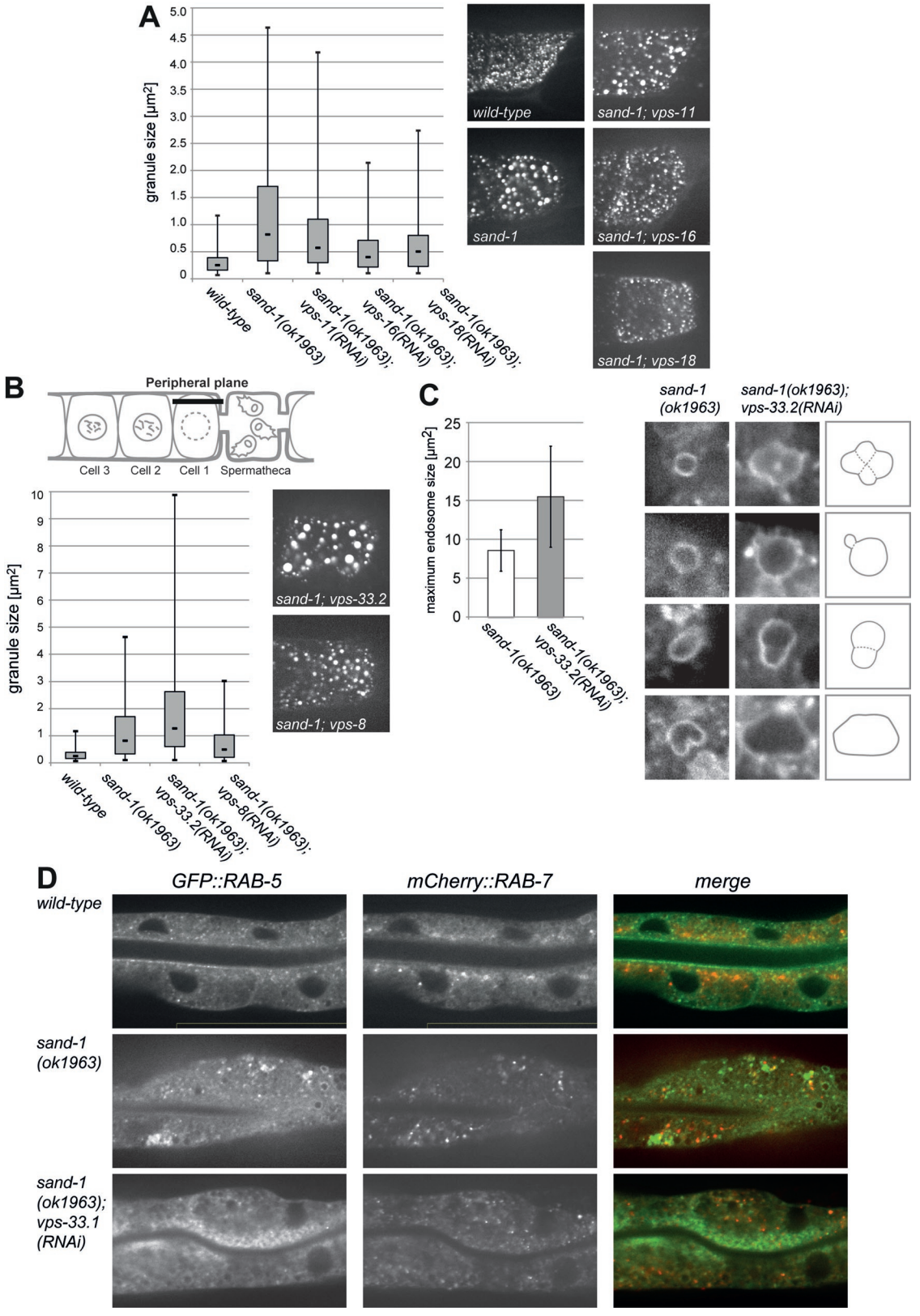

FIGURE 6: CORVET is responsible for the enlarged endosomes found in *sand-1* worms, and its VPS-33.2 subunit ensures fusion specificity. (A, B) Yolk granule size in the indicated worms was measured in the oocyte most proximal to the spermatheca (see *Materials and Methods* for a detailed description). Schematic view in B shows peripheral plane used for yolk granule size measurements. (A) Knockdown of core subunits *vps-11*, *vps-16*, and *vps-18* causes reduction of *sand-1(ok1963)* yolk granule size ($p = 1.3E-5$ for *vps-11*, $p = 2.4E-21$ for *vps-16*, $p = 4.2E-16$ for *vps-18* compared with *sand-1*). Representative cell pictures show a top view of the cells in which the peripheral localization of granules (Figure 5A) cannot be seen. (B) RNAi of CORVET subunit *vps-8* leads to smaller vesicles ($p = 9.8E-9$ compared with

degradation of soluble secreted GFP (Figure 8C) to a similar time frame that we had reported for wild type (Poteryaev *et al.*, 2007).

Taken together, our data suggest a role of the SM proteins VPS-33.1 and VPS-33.2 in fusion specificity along the endosomal pathway. In their absence, fusion may happen in a less restricted manner, allowing the bypass of the endosomal transport block in *sand-1* mutants.

DISCUSSION

Here we reveal the existence of HOPS and CORVET tethering complexes in metazoans. Although the presence of a metazoan HOPS complex had been suggested by a number of groups (Akbar *et al.*, 2011; Balderhaar and Ungermann, 2013; Graham *et al.*, 2013; Klinger *et al.*, 2013; Tornieri *et al.*, 2013; Pols *et al.*, 2013a), we provide the first systematic study on these two tethering complexes. This type of analysis is important because at least hVps41 also appears to have a function independent of the HOPS complex (Pols *et al.*, 2013b). Thus other members of these tethering complexes also may have a different function in the cell. We found homologues of all the HOPS components, but we did not identify a Vps3 homologue in *C. elegans*, which is a CORVET-specific subunit (Solinger and Spang, 2013). In contrast, *C. elegans* and other metazoans contain two homologues of the SM protein Vps33. VPS-33.1 is present in the HOPS complex, and VPS-33.2 is the CORVET-specific subunit in *C. elegans*. This complex organization is likely also maintained in mammals, but this remains to be determined. Metazoans also contain two homologues of the core component Vps16, VPS-16 and SPE-39. Of importance, VPS-16 is the direct interaction partner of the SM subunit (Lobingier and Merz, 2012; Baker *et al.*, 2013; Balderhaar and Ungermann, 2013; Graham *et al.*, 2013). Mammalian Vps33b appears to interact with the second Vps16 subunit (Tornieri *et al.*, 2013). Our data indicate VPS-33.2, which would be the orthologue of Vps33b, as a CORVET-specific subunit. However, more CORVET/HOPS-type tethering complexes may exist. For example *vps-8(RNAi)* and *vps33-2(RNAi)* have a yolk uptake defect, which is not observed after silencing of the core subunits. It is conceivable that SPE-39 would replace VPS-16 in this complex. Another possibility is that subcomplexes of the tethers are sufficient to promote tethering functions. This possibility seems unlikely, given the requirement of the entire HOPS complex for homotypic vacuolar fusion (Ostrowicz *et al.*, 2010). We also cannot exclude moonlighting functions of VPS-8 and VPS-33.2 in yolk uptake. However, populations of mixed CORVET/HOPS complexes were observed in yeast (Peplowska *et al.*, 2007). Thus it is plausible that VPS-16 and its homologue SPE-39 can individually interact with several SM proteins on one side and with different core components on the other. Therefore multiple HOPS/CORVET-like tethering complexes might exist in the endosomal system that could assemble in a Lego-like organization, depending on which membranes they would have to tether.

Our results indicate that the CORVET complex acts upstream and the HOPS downstream or at the same level of Rab conversion from RAB-5– to RAB-7–positive endosomes (Figure 9A). These findings are consistent with the proposed roles for both tethering complexes in yeast (Wickner, 2010; Balderhaar *et al.*, 2013; Balderhaar and Ungermann, 2013; Epp and Ungermann, 2013; Zick and Wickner, 2013). Of interest, knockdown of CORVET components resulted in accumulation of RAB-5 at the apical cortex and recruitment of RAB-7 onto endosomes in gut epithelial cells, indicating that the CORVET complex may play a role in stabilizing RAB-5 on endosomes (Figure 9B). Alternatively, in the absence of the CORVET complex, the HOPS complex could be recruited prematurely, driving Rab conversion. We consider the latter possibility less likely because knockdown of the core components, which are shared between the two complexes, resulted in the same phenotype as silencing of the CORVET-specific subunits. Consistent with CORVET acting upstream of Rab conversion, RAB-5–positive endosomes remained small and were still more apically localized in *sand-1(ok1963) vps-8(RNAi)*.

Conversely, loss of the HOPS-specific subunits may bring about delayed Rab conversion and hence endosome maturation, as RAB-5 stayed on RAB-7–positive endosomes that had migrated toward the cell center and the basal side of the epithelial cells (Figure 9B), consistent with the notion of CORVET being involved in stabilization of RAB-5 on endosomes. In the absence of HOPS, RAB-7 could be recruited by SAND-1/CCZ-1 but may not be able to displace RAB-5. The HOPS complex may be actively involved in RAB-5 displacement from endosomes. Thus, in the way in which CORVET would participate in the stabilization of RAB-5 on endosomes, HOPS could stabilize RAB-7.

In addition to this collaboration of CORVET and HOPS with the Rab switch complex SAND-1/CCZ-1, we also observed instances of mislocalization or mistrafficking of endosomes, suggesting involvement of these complexes in cytoskeleton interactions (Figures 2G, 3A, and 5C). CORVET and HOPS subunits interact with microtubules and actin to affect the localization of endosomal compartments in mammals (Poupon *et al.*, 2003; Richardson *et al.*, 2004; Xu *et al.*, 2008). Thus our observation suggests coordination between membrane tethering/fusion, Rab conversion, and transport/localization during endosome maturation.

When we silenced the CORVET-specific SM protein VPS-33.2 in *sand-1(ok1963)* oocytes, we observed an increase in the size of yolk-positive internal structures. Similarly, in *vps-33.2(RNAi) sand-1(ok1963)* coelomocytes, BSA-TR accumulated in bigger internal structures than observed under the same conditions in *sand-1(ok1963)* alone. However, because it is a CORVET-specific SM protein, fusion should be inhibited and only small endocytic structures should be observed in both organs, as for *vps-8(RNAi)*. We propose that in the absence of VPS-33.2, VPS-33.1 could be incorporated into the CORVET complex, promoting fusion with a wrong compartment, or, since it is a noncognate SM protein, fusion may be stalled after fusion pore opening. Similarly, silencing of the HOPS-specific VPS-33.1 might allow VPS-33.2 to fill in as part of the HOPS complex, again compromising fusion specificity. We consider the existence of tethering complexes that would contain the RAB-5

sand-1), whereas *vps-33.2* shows further enlargement of *sand-1(ok1963)* vesicles ($p = 5.9E\text{-}9$ compared with *sand-1*; note the different scales on the *y*-axes in A and B). Corresponding wild-type and *sand-1* oocytes are shown in A. (C) *vps-33.2(RNAi)* causes enlargement of RAB-5 compartment in *sand-1(ok1963)* intestinal cells (see also Figure 5B, bottom). Only the largest vesicles in each gut were measured ($N = 25$). Vesicles in *sand-1(ok1963); vps-33.2(RNAi)* are significantly bigger ($p = 2.5E\text{-}5$). Examples are shown on the right, with schematic drawings of irregularly shaped and partially fused "supersize" vesicles below. (D) GFP::RAB-5 localization near the gut lumen in *sand-1(ok1963); vps-33.1(RNAi)* worms, with mCherry::RAB-7 compartment similar to *sand-1* alone, corresponding wild-type and *sand-1* worms area shown for comparison.

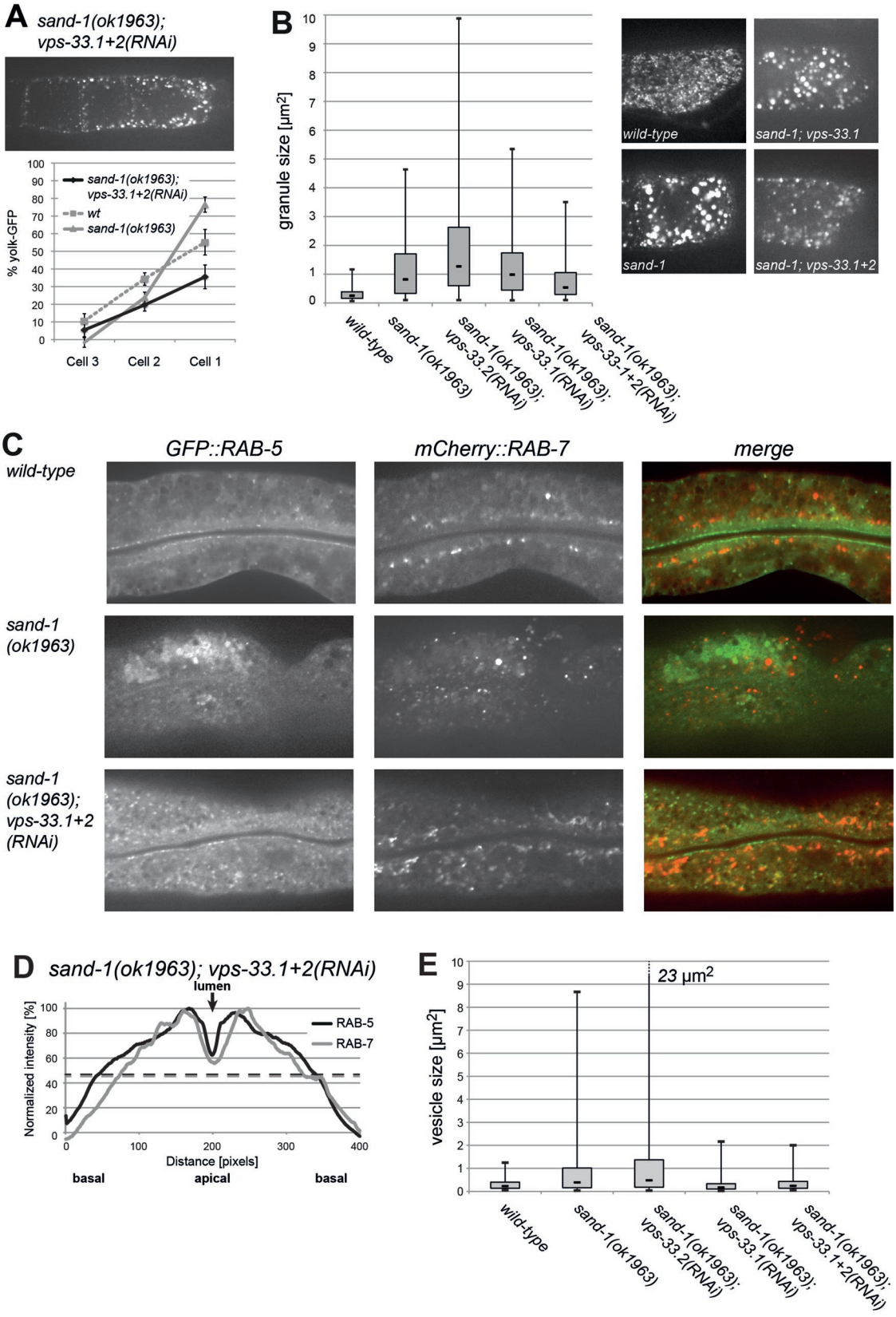

FIGURE 7: Loss of specificity by concomitant knockdown of *vps-33.1* and *vps-33.2* leads to suppression of the *sand-1* phenotype. (A) YP170-GFP uptake in *sand-1(ok1963); vps-33.1(RNAi); vps-33.2(RNAi)* oocytes (see legend to Figure 1 for detailed description). (B) Yolk granule size is reduced in *sand-1(ok1963); vps-33.1+2(RNAi)* worms ($p = 7.6E-9$ compared with *sand-1*; for detailed description, see *Materials and Methods*). (C) *sand-1(ok1963); vps-33.1+2(RNAi)* worms show a partial suppression of *sand-1* defects (compared with wild-type and *sand-1* shown above). (D) Profile plot across *vps-33.1+2(RNAi)* guts (see Figure 2G for description and comparison to wild-type and *sand-1* worms). (E) RAB-5

			Mock	Core	*vps-33.1+2*
Oocytes	*sand-1*	Yolk	(Peripheral), enlarged	Peripheral, small	(Peripheral), small
Gut	*sand-1*	RAB-5	Central, enlarged	Apical, small	Wild type, small
		RAB-7	Dispersed	Dispersed	Organized, (compartment)
	wild-type	hTfR	Near apical, few large basal	Apical + basal accumulation	Disorganized
	sand-1	hTfR	Central, aggregated	Apical	Dispersed, (few large basal)

Localization of vesicles/granules is described, and size is indicated in those cases in which it was measured. The descriptions in parentheses indicate a weak phenotype.

TABLE 2: Differences between knockdowns of core subunits and *vps-33.1+2*.

interacting component of the CORVET and the SM protein of the HOPS or vice versa a rather plausible scenario. In yeast, CORVET and HOPS appear to exist in a dynamic equilibrium in which the Rab-interacting members of the complexes are interchangeable (Peplowska *et al*., 2007). In the *sand-1* mutant, loss of the HOPS-specific SM protein would result in a complex that contains the RAB-7–interacting subunits and the CORVET SM protein. This complex would be nonfunctional, as RAB-7 was not recruited onto late endosomes. As a consequence, VPS-33.2 levels present incorporated in a bona fide CORVET complex may be too low and hence give the same phenotype as knockdown of the CORVET subunit VPS-8. This scenario is rather probable, as mutations in yeast *VPS33* that reduced the ability of Vps33 to assemble into the HOPS complex also showed mislocalization vacuolar proteins and displayed vacuolar morphology defects (Lobingier and Merz, 2012).

Of interest, concomitant loss of both SM proteins partially rescued transport down to the lysosome in *sand-1(-/-)*. Thus the requirement for SAND-1 in lysosomal transport was bypassed (Figure 9C). Although we recover in part the endosomal organization, cellular functions are still compromised, and the survival rate of *sand-1(ok1963)* worms was not improved by silencing both VPS-33 forms.

We propose a model in which the SM proteins VPS-33.1 and VPS-33.2, together with the Rab interactors of the tethering complexes, ensure vectorial transport through the endosomal system. In the absence of both SM proteins, control of SNARE pairing would be reduced and fusion specificity negatively affected. Fusion pore opening depends on Vps33 in contact with cognate target-SNARE (Pieren *et al*., 2010). In yeast, there is only one Vps33 protein, which might be more promiscuous. In higher eukaryotes, which have two Vps33 isoforms, the interaction with the SNAREs might be more restrictive. In fact in *Drosophila*, such specificity has been reported for the Vps33 isoforms (Akbar *et al*., 2009). In support of this notion, the human ARC syndrome is specifically caused by mutations in VPS33B (*C. elegans* VPS-33.2; Smith *et al*., 2012). Similarly, mutations in VPS33A (*C. elegans* VPS-33.1) results in Hermansky–Pudlak syndrome (Guo *et al*., 2009), in which fusion of multivesicular bodies with lysosomes is impaired. It is possible that CORVET and HOPS complexes under those conditions would lack any SM protein. The yeast HOPS complex lacking Vps33 is inactive and shows a strong vacuole phenotype (type C, which is the complete lack of a vacuole; Raymond *et al*., 1992). Even a reduction of Vps33 interaction with the complex already causes perturbations in trafficking (Lobingier and Merz, 2012). It is therefore unlikely that HOPS can work without an SM subunit. The most likely candidate to fill the empty SM protein position is the closely related VPS-45 protein. It shares significant sequence homology with both VPS-33.1 and VPS-33.2 and has been implicated in tethering events in the endosomal pathway (VPS-33.1 and VPS-33.2 share 37% similarity, and VPS-45 has 36–37% similarity with the two SM proteins; see also Solinger and Spang, 2013). It is conceivable that VPS-45 could replace the missing VPS-33 protein in the single-knockdown experiments. Of interest, the mutated residues in yeast Vps33, which caused dissociation from the complex (Lobingier and Merz, 2012), are located mostly in highly conserved regions between the VPS-33 and VPS-45 proteins. This might indicate that the interaction surfaces between the SM proteins and the CORVET or HOPS complex are similar enough to accommodate different combinations of tethering and specificity factors.

Mon1/Ccz1 was shown to act as a guanine nucleotide exchange factor (GEF) for Ypt7/Rab7 in yeast (Nordmann *et al*., 2010). Surprisingly, RAB-7 is recruited on membranes in *sand-1(ok1963) vps-33.1+2(RNAi)*, suggesting the presence of another RAB-7 GEF besides SAND-1/CCZ-1 in *C. elegans*.

Transport through the endosomal system is strongly regulated by the tethering complexes CORVET and HOPS, and our data indicate the presence of more tethering complexes of this type. The reason for this expansion of the complexes might be the increase in complexity from yeast to metazoans. Different types of early and late endosomes have been described in mammalian cells (Grant and Donaldson, 2009; Marks *et al*., 2013). Employing a Lego-like system makes these tethering complexes uniquely versatile and allows quick adaptation to the amount and type of endocytic flux in the cell.

MATERIALS AND METHODS

General methods and strains

Worm cultures, genetic crosses, and other *C. elegans* general methods were performed according to standard protocols (Brenner, 1974). All worms were grown at 20°C, at which *sand-1(ok1963)* worms are viable but still show severe endosomal trafficking defects (Poteryaev *et al*., 2007).

The following *C. elegans* strains and transgenes were used: *vps-18(tm1125)II*, *sand-1(ok1963)IV*, *bIs1[YP170::GFP + rol-6(su1006)]X*, *pwIs429[vha-6::mCherry-rab-7]*, *pwIs72[vha6p::GFP::rab-5 + unc-119(+)]*,*pwIs90[Pvha-6::hTfR-GFP; Cbr-unc-119(+)]*, *pwIs50[lmp-1::GFP + Cb-unc-119(+)]*, *and pwIs518[vha-6::GFP-HGRS-1]*.

vesicles in *sand-1; vps-33.1+2* double-knockdown worms are wild-type size. Plots show 25th–75th percentile box, with median and whiskers indicating minimal and maximal values (the maximal value for *sand-1, vps-33.2* was shortened for clarity). Vesicles in *sand-1* are significantly larger than in wild type (p = 5.7E-31), *sand-1; vps-33.2* vesicles are bigger than *sand-1* alone (p = 1.6E-6), whereas *sand-1; vps-33.1* (p = 0.06) and *sand-1; vps-33.1+2* (p = 0.14) are the same as wild type.

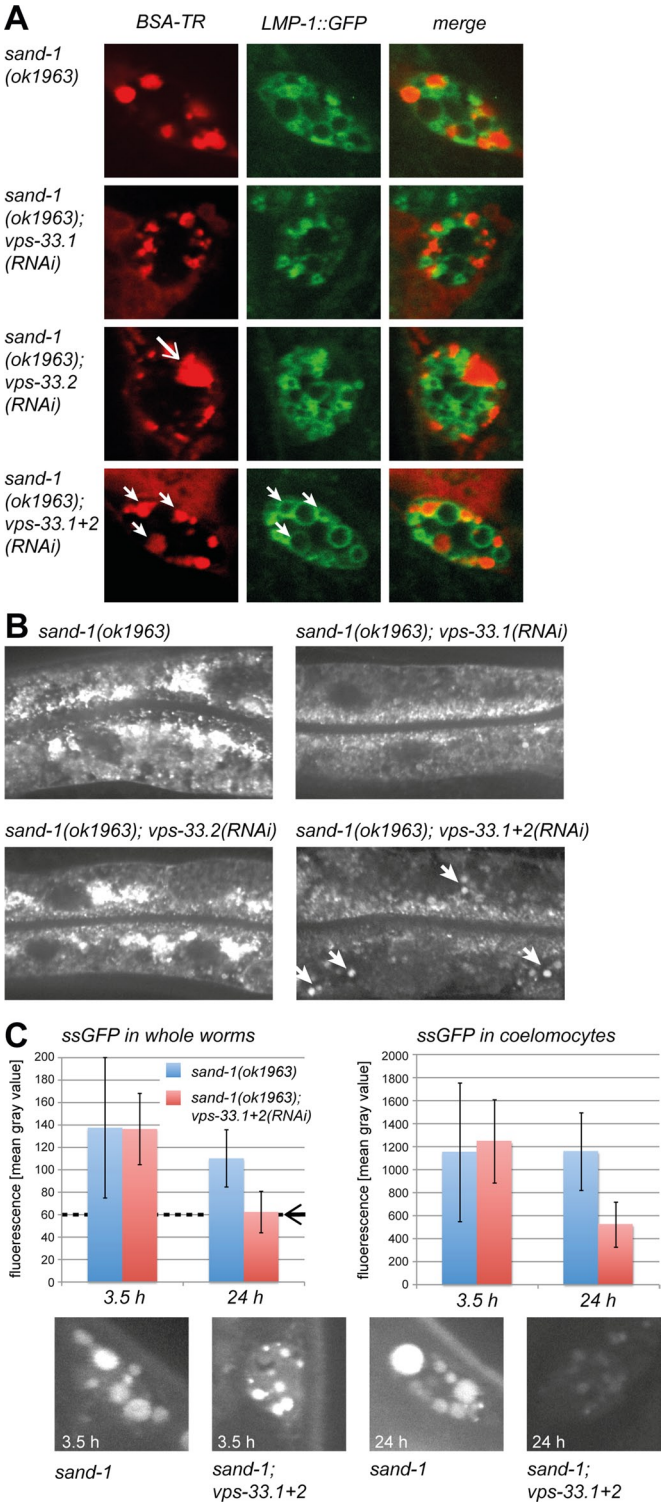

FIGURE 8: Bypass of *sand-1(ok1963)* block by knockdown of *vps-33.1* and *vps-33.2*. (A) Localization of BSA-TR 30 min after injection compared with the lysosomal marker LMP-1. Shown are representative coelomocytes for the indicated strains. Colocalization in *sand-1* alone and single knockdowns was usually in only one vesicle. The large arrow indicates an enlarged compartment in *vps-33.2(RNAi)*; small arrows point to lysosomes (positive for LMP-1::GFP) containing BSA-TR in the *vps-33.1+2(RNAi)* coelomocyte. (B) Lysosomal compartments are partially re-formed in *sand-1(ok1963)* worms with a *vps-33.1+2* knockdown. Abnormal lysosomal compartment in *sand-1(ok1963)* intestine with large vesicle aggregations in the center of the cells and absence of large basal lysosomes. Knockdown of *vps-33.1* causes formation of small vesicles near the gut lumen. Phenotype similar to *sand-1(ok1963)* is seen in *vps-33.2(RNAi)* intestine. Double knockdown of *vps-33.1+2* allows formation of large late endosomes/lysosomes located on the basal side of the cells (indicated by arrows). (C) Soluble secreted GFP (ssGFP) is degraded in *sand-1; vps-33.1+2* double-knockdown coelomocytes. GFP fluorescence was measured in whole worms and coelomocytes 3.5 and 24 h after heat shock (30 min at 33°C). The arrow and dashed line indicate the background fluorescence in the whole worms. Representative coelomocytes are shown at the bottom. After 24 h, ssGFP fluorescence was significantly lower in *sand-1; vps-33.1+2* compared with *sand-1* alone in the whole worms ($p = 0.00018$) and coelomocytes ($p = 0.00013$; $N = 10$).

RNAi by feeding was performed for 3 d starting from L1 larvae and was carried out using sequenced and confirmed clones from the Ahringer library (Kamath *et al.*, 2003).

GFP tagging of *vps-33.1* and *vps-33.2*

Promoter, open reading frame (ORF), and terminator sequences of *vps-33.1* and *vps-33.2* genes were cloned into the pCFJ151 plasmid (Frøkjaer-Jensen *et al.*, 2008). ORF and 5′ upstream intergenic regions of *vps-33.1* and *vps-33.2* were cloned into *Avr*II-*Sbf*I. GFP was obtained from pJA257 plasmid (from Addgene, Cambridge, MA; Julie Ahringer lab) and cloned into *Xho*I-*Bsi*WI. The 3′ downstream intergenic region with putative terminator was cloned into *Bsi*WI-*Bss*HII. Worm lines were obtained according to MosSCI protocol (Frøkjaer-Jensen *et al.*, 2008). Putative single- copy integrated lines showed no visible GFP signal, probably because of low expression from the *vps-33.1* and *vps-33.2* promoters. Lines bearing extrachromosomal arrays were analyzed and showed mosaic expression in different cell types, including intestine (Figure 1B), coelomocytes, neurons, muscles, and seam cells.

Microscopy

Live worms, immobilized with 20 mM levamisole in M9, were mounted on agarose pads cast on microscopy slides. The worms were imaged with a spinning-disk confocal system Andor Revolution (Andor Technologies, Belfast, Northern Ireland) mounted onto an IX-81 inverted microscope (Olympus, Center Valley, PA) equipped with an iXon^{EM}+ electron-multiplying charge-coupled device camera (Andor Technologies). Specimens were imaged using a 63×/1.42 numerical aperture oil objective. Each pixel represents 0.107 µm. Excitation was achieved using solid-state 488- and 560-nm lasers. Exposure time was 100 ms. Each image was a result of four averaged frames for oocytes and 32 averaged frames for intestine and coelomocytes. Images were all processed in the same way for corresponding experiments.

For YP170::GFP quantification, *z*-stacks were taken with identical settings (laser 488 nm at 10% output, 0.1 s exposure. and four averaged frames/picture). Wild-type and *sand-1(ok1963)* worms were quantified for each series of experiments to ensure the proper performance of the imaging system, and the results were very reproducible. The curves shown in all figures with oocytes are paired with the corresponding wild-type and *sand-1* controls taken in the same series of experiments.

Granule size measurements

Oocytes with nicely separated granules were chosen for the analysis in ImageJ (National Institutes of Health, Bethesda, MD). Pictures were transformed into binary by using the threshold function. Close

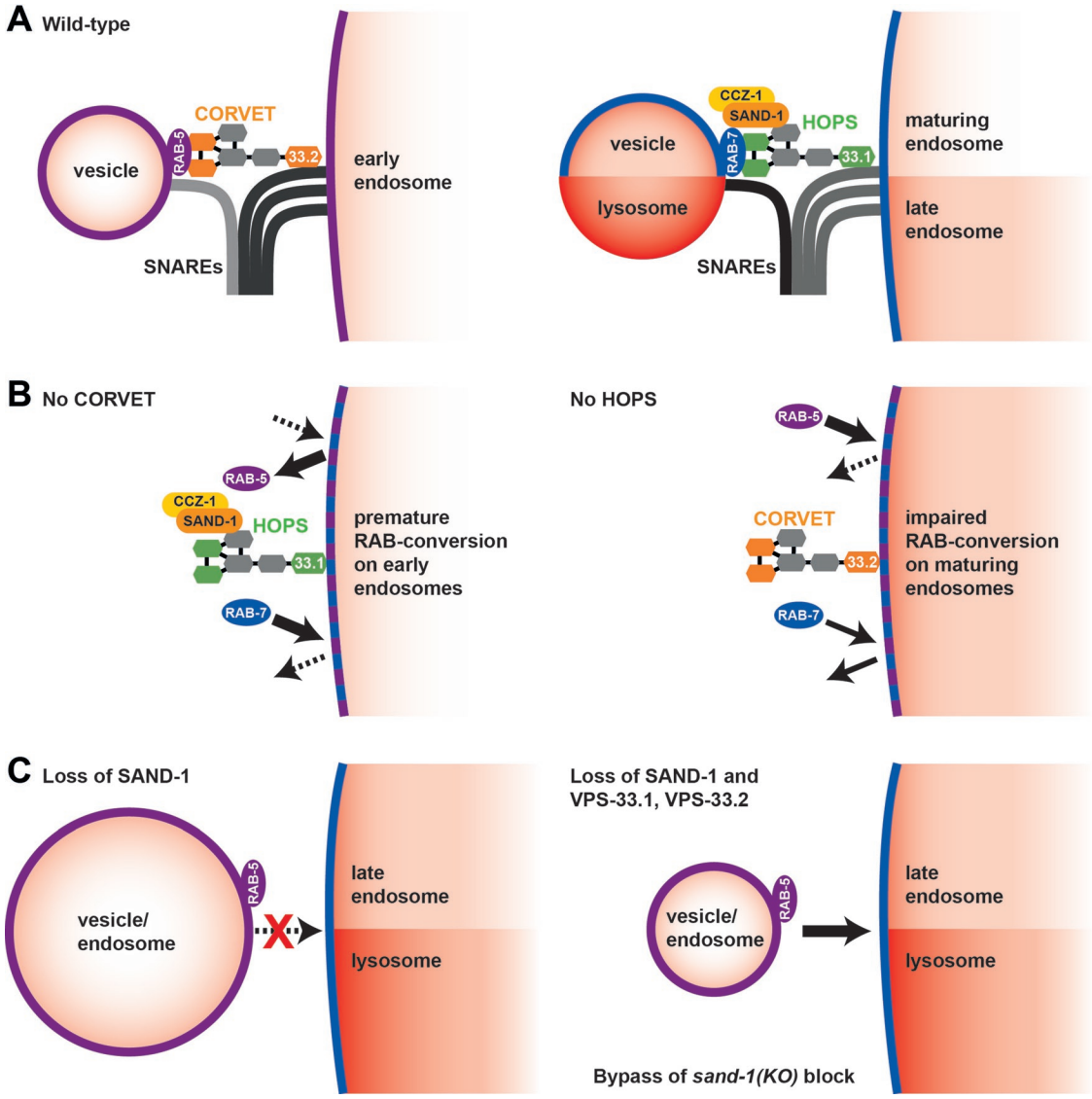

FIGURE 9: Model for CORVET and HOPS function in vesicle fusion and RAB conversion. (A) Role of CORVET in tethering and ensuring fusion specificity on early endosomes. Function of HOPS together with SAND-1 in tethering and allowing fusion of late endosomes/lysosomes. (B) Effects of CORVET and HOPS complexes on RAB conversion. Premature RAB conversion in the absence of CORVET: untimely recruitment of SAND-1/CCZ-1 leads to small early endosomes with RAB-7. Impaired RAB-conversion in the absence of HOPS: lost ability to properly bind SAND-1/CCZ-1 causes a failure to remove RAB-5 and leads to enlarged mixed compartments near basal side of cells bearing both RAB-5 and RAB-7. (C) Bypass of *sand-1* block in the absence of CORVET and HOPS-specific SM proteins.

and watershed functions were applied to ensure that all granules were separated (this also eliminates single-pixel noise). Granule sizes were measured in a region of interest containing cell 1 using analyze particle (circularity settings, 0.0–0.8). Outlines were checked to ensure that only proper vesicles were measured. Wild-type cells contained ~80–100 vesicles/cell and *sand-1* cells ~30–50 vesicles. Vesicle sizes in the gut were measured in the same way.

Pulse chase

The traffic of BSA-TR in coelomocytes was monitored as described previously (Poteryaev *et al.*, 2007). Bypass of the *sand-1* block was monitored at 20°C. For each condition, ≥20 different worms were analyzed. Traffic of BSA-TR in wild-type worms was as described (Poteryaev *et al.*, 2007).

ACKNOWLEDGMENTS

We thank the *Caenorhabditis* Genetic Center for strains, K. Ackema for critical reading of the manuscript, and Ian G. Macara for helpful suggestions. This study was supported by the University of Basel and the Swiss National Science Foundation (Sinergia Grant CRSII3_141956).

REFERENCES

Abenza JF, Galindo A, Pantazopoulou A, Gil C, de los Ríos V, Peñalva MA (2010). Aspergillus RabB Rab5 integrates acquisition of degradative identity with the long distance movement of early endosomes. Mol Biol Cell 21, 2756–2769.

Ackema KB, Sauder U, Solinger JA, Spang A (2013). The ArfGEF GBF-1 is required for ER structure, secretion and endocytic transport in C. elegans. PLoS One 8, e67076.

Akbar MA, Ray S, Krämer H (2009). The SM protein Car/Vps33A regulates SNARE-mediated trafficking to lysosomes and lysosome-related organelles. Mol Biol Cell 20, 1705–1714.
Akbar MA, Tracy C, Kahr WHA, Krämer H (2011). The full-of-bacteria gene is required for phagosome maturation during immune defense in Drosophila. J Cell Biol 192, 383–390.
Baker RW, Jeffrey PD, Hughson FM (2013). Crystal structures of the Sec1/Munc18 (SM) protein Vps33, alone and bound to the homotypic fusion and vacuolar protein sorting (HOPS) subunit Vps16*. PLoS One 8, e67409.
Balderhaar HJK, Lachmann J, Yavavli E, Bröcker C, Lürick A, Ungermann C (2013). The CORVET complex promotes tethering and fusion of Rab5/Vps21-positive membranes. Proc Natl Acad Sci USA 110, 3823–3828.
Balderhaar HJK, Ungermann C (2013). CORVET and HOPS tethering complexes—coordinators of endosome and lysosome fusion. J Cell Sci 126, 1307–1316.
Besterman JM, Low RB (1983). Endocytosis: a review of mechanisms and plasma membrane dynamics. Biochem J 210, 1–13.
Brenner S (1974). The genetics of Caenorhabditis elegans. Genetics 77, 71–94.
Bröcker C, Kuhlee A, Gatsogiannis C, Balderhaar HJK, Hönscher C, Engelbrecht-Vandré S, Ungermann C, Raunser S (2012). Molecular architecture of the multisubunit homotypic fusion and vacuole protein sorting (HOPS) tethering complex. Proc Natl Acad Sci USA 109, 1991–1996.
Chen CC-H, Schweinsberg PJ, Vashist S, Mareiniss DP, Lambie EJ, Grant BD (2006). RAB-10 is required for endocytic recycling in the Caenorhabditis elegans intestine. Mol Biol Cell 17, 1286–1297.
Chotard L, Mishra AK, Sylvain M-A, Tuck S, Lambright DG, Rocheleau CE (2010). TBC-2 regulates RAB-5/RAB-7-mediated endosomal trafficking in Caenorhabditis elegans. Mol Biol Cell 21, 2285–2296.
Epp N, Ungermann C (2013). The N-terminal domains of Vps3 and Vps8 are critical for localization and function of the CORVET tethering complex on endosomes. PLoS One 8, e67307.
Fares H, Greenwald I (2001a). Genetic analysis of endocytosis in Caenorhabditis elegans: coelomocyte uptake defective mutants. Genetics 159, 133–145.
Fares H, Greenwald I (2001b). Regulation of endocytosis by CUP-5, the Caenorhabditis elegans mucolipin-1 homolog. Nat Genet 28, 64–68.
Frøkjaer-Jensen C, Davis MW, Hopkins CE, Newman BJ, Thummel JM, Olesen S-P, Grunnet M, Jorgensen EM (2008). Single-copy insertion of transgenes in Caenorhabditis elegans. Nat Genet 40, 1375–1383.
Furgason MLM, MacDonald C, Shanks SG, Ryder SP, Bryant NJ, Munson M (2009). The N-terminal peptide of the syntaxin Tlg2p modulates binding of its closed conformation to Vps45p. Proc Natl Acad Sci USA 106, 14303–14308.
Gengyo-Ando K, Kuroyanagi H, Kobayashi T, Murate M, Fujimoto K, Okabe S, Mitani S (2007). The SM protein VPS-45 is required for RAB-5-dependent endocytic transport in Caenorhabditis elegans. EMBO Rep 8, 152–157.
Gissen P, Johnson CA, Gentle D, Hurst LD, Doherty AJ, O'Kane CJ, Kelly DA, Maher ER (2005). Comparative evolutionary analysis of VPS33 homologues: genetic and functional insights. Hum Mol Genet 14, 1261–1270.
Graham SC, Wartosch L, Gray SR, Scourfield EJ, Deane JE, Luzio JP, Owen DJ (2013). Structural basis of Vps33A recruitment to the human HOPS complex by Vps16. Proc Natl Acad Sci USA 110, 13345–13350.
Grant BD, Donaldson JG (2009). Pathways and mechanisms of endocytic recycling. Nat Rev Mol Cell Biol 10, 597–608.
Grant B, Hirsh D (1999). Receptor-mediated endocytosis in the Caenorhabditis elegans oocyte. Mol Biol Cell 10, 4311–4326.
Guo X, Tu L, Gumper I, Plesken H, Novak EK, Chintala S, Swank RT, Pastores G, Torres P, Izumi T, *et al.* (2009). Involvement of vps33a in the fusion of uroplakin-degrading multivesicular bodies with lysosomes. Traffic 10, 1350–1361.
Hermann GJ, Schroeder LK, Hieb CA, Kershner AM, Rabbitts BM, Fonarev P, Grant BD, Priess JR (2005). Genetic analysis of lysosomal trafficking in Caenorhabditis elegans. Mol Biol Cell 16, 3273–3288.
Huizing M, Didier A, Walenta J, Anikster Y, Gahl WA, Krämer H (2001). Molecular cloning and characterization of human VPS18, VPS 11, VPS16, and VPS33. Gene 264, 241–247.
Huotari J, Helenius A (2011). Endosome maturation. EMBO J 30, 3481–3500.
Kamath RS, Fraser AG, Dong Y, Poulin G, Durbin R, Gotta M, Kanapin A, Le Bot N, Moreno S, Sohrmann M, *et al.* (2003). Systematic functional analysis of the Caenorhabditis elegans genome using RNAi. Nature 421, 231–237.
Kinchen JM, Doukoumetzidis K, Almendinger J, Stergiou L, Tosello-Trampont A, Sifri CD, Hengartner MO, Ravichandran KS (2008). A pathway for phagosome maturation during engulfment of apoptotic cells. Nat Cell Biol 10, 556–566.
Kinchen JM, Ravichandran KS (2010). Identification of two evolutionarily conserved genes regulating processing of engulfed apoptotic cells. Nature 464, 778–782.
Klinger CM, Klute MJ, Dacks JB (2013). Comparative genomic analysis of multi-subunit tethering complexes demonstrates an ancient pan-eukaryotic complement and sculpting in apicomplexa. PLoS One 8, e76278.
Lobingier BT, Merz AJ (2012). Sec1/Munc18 protein Vps33 binds to SNARE domains and the quaternary SNARE complex. Mol Biol Cell 23, 4611–4622.
Marks MS, Heijnen HFG, Raposo G (2013). Lysosome-related organelles: unusual compartments become mainstream. Curr Opin Cell Biol 25, 495–505.
Morrison HA, Dionne H, Rusten TE, Brech A, Fisher WW, Pfeiffer BD, Celniker SE, Stenmark H, Bilder D (2008). Regulation of early endosomal entry by the Drosophila tumor suppressors Rabenosyn and Vps45. Mol Biol Cell 19, 4167–4176.
Nickerson DP, Brett CL, Merz AJ (2009). Vps-C complexes: gatekeepers of endolysosomal traffic. Curr Opin Cell Biol 21, 543–551.
Nicot A-S, Fares H, Payrastre B, Chisholm AD, Labouesse M, Laporte J (2006). The phosphoinositide kinase PIKfyve/Fab1p regulates terminal lysosome maturation in Caenorhabditis elegans. Mol Biol Cell 17, 3062–3074.
Nordmann MM, Cabrera MM, Perz AA, Bröcker CC, Ostrowicz CC, Engelbrecht-Vandré SS, Ungermann CC (2010). The Mon1-Ccz1 complex is the GEF of the late endosomal Rab7 homolog Ypt7. Curr Biol 20, 1654–1659.
Ostrowicz CW, Bröcker C, Ahnert F, Nordmann M, Lachmann J, Peplowska K, Perz A, Auffarth K, Engelbrecht-Vandré S, Ungermann C (2010). Defined subunit arrangement and rab interactions are required for functionality of the HOPS tethering complex. Traffic 11, 1334–1346.
Parker S, Walker DS, Ly S, Baylis HA (2009). Caveolin-2 is required for apical lipid trafficking and suppresses basolateral recycling defects in the intestine of Caenorhabditis elegans. Mol Biol Cell 20, 1763–1771.
Peplowska K, Markgraf DF, Ostrowicz CW, Bange G, Ungermann C (2007). The CORVET tethering complex interacts with the yeast Rab5 homolog Vps21 and is involved in endo-lysosomal biogenesis. Dev Cell 12, 739–750.
Pieren M, Schmidt A, Mayer A (2010). The SM protein Vps33 and the t-SNARE H(abc) domain promote fusion pore opening. Nat Struct Mol Biol 17, 710–717.
Plemel RL, Lobingier BT, Brett CL, Angers CG, Nickerson DP, Paulsel A, Sprague D, Merz AJ (2011). Subunit organization and Rab interactions of Vps-C protein complexes that control endolysosomal membrane traffic. Mol Biol Cell 22, 1353–1363.
Pols MS, Brink ten C, Gosavi P, Oorschot V, Klumperman J (2013a). The HOPS proteins hVps41 and hVps39 are required for homotypic and heterotypic late endosome fusion. Traffic 14, 219–232.
Pols MS, van Meel E, Oorschot V, Brink ten C, Fukuda M, Swetha MG, Mayor S, Klumperman J (2013b). hVps41 and VAMP7 function in direct TGN to late endosome transport of lysosomal membrane proteins. Nat Commun 4, 1361.
Poteryaev D, Datta S, Ackema K, Zerial M, Spang A (2010). Identification of the switch in early-to-late endosome transition. Cell 141, 497–508.
Poteryaev DD, Fares HH, Bowerman BB, Spang AA (2007). Caenorhabditis elegans SAND-1 is essential for RAB-7 function in endosomal traffic. EMBO J 26, 301–312.
Poupon V, Stewart A, Gray SR, Piper RC, Luzio JP (2003). The role of mVps18p in clustering, fusion, and intracellular localization of late endocytic organelles. Mol Biol Cell 14, 4015–4027.
Pryor PRP, Luzio JPJ (2009). Delivery of endocytosed membrane proteins to the lysosome. Biochim Biophys Acta 1793, 615–624.
Pulipparacharuvil S, Akbar MA, Ray S, Sevrioukov EA, Haberman AS, Rohrer J, Krämer H (2005). Drosophila Vps16A is required for trafficking to lysosomes and biogenesis of pigment granules. J Cell Sci 118, 3663–3673.
Rahajeng J, Caplan S, Naslavsky N (2010). Common and distinct roles for the binding partners Rabenosyn-5 and Vps45 in the regulation of endocytic trafficking in mammalian cells. Exp Cell Res 316, 859–874.
Raymond CK, Howald-Stevenson I, Vater CA, Stevens TH (1992). Morphological classification of the yeast vacuolar protein sorting mutants: evidence for a prevacuolar compartment in class E vps mutants. Mol Biol Cell 3, 1389–1402.

Richardson SCW, Winistorfer SC, Poupon V, Luzio JP, Piper RC (2004). Mammalian late vacuole protein sorting orthologues participate in early endosomal fusion and interact with the cytoskeleton. Mol Biol Cell 15, 1197–1210.
Rink J, Ghigo E, Kalaidzidis Y, Zerial M (2005). Rab conversion as a mechanism of progression from early to late endosomes. Cell 122, 735–749.
Roudier N, Lefebvre C, Legouis R (2005). CeVPS-27 is an endosomal protein required for the molting and the endocytic trafficking of the low-density lipoprotein receptor-related protein 1 in Caenorhabditis elegans. Traffic 6, 695–705.
Ruaud A-F, Nilsson L, Richard F, Larsen MK, Bessereau J-L, Tuck S (2009). The C. elegans P4-ATPase TAT-1 regulates lysosome biogenesis and endocytosis. Traffic 10, 88–100.
Sato M, Sato K, Fonarev P, Huang C-J, Liou W, Grant BD (2005). Caenorhabditis elegans RME-6 is a novel regulator of RAB-5 at the clathrin-coated pit. Nat Cell Biol 7, 559–569.
Seals DF, Eitzen G, Margolis N, Wickner WT, Price A (2000). A Ypt/Rab effector complex containing the Sec1 homolog Vps33p is required for homotypic vacuole fusion. Proc Natl Acad Sci USA 97, 9402–9407.
Smith H, Galmes R, Gogolina E, Straatman-Iwanowska A, Reay K, Banushi B, Bruce CK, Cullinane AR, Romero R, Chang R, *et al.* (2012). Associations among genotype, clinical phenotype, and intracellular localization of trafficking proteins in ARC syndrome. Hum Mutat 33, 1656–1664.
Solinger JA, Poteryaev D, Spang A (2014). Application of RNAi technology and fluorescent protein markers to study membrane traffic in C. elegans. Methods Mol Biol 1174, 329–347.
Solinger JA, Spang A (2013). Tethering complexes in the endocytic pathway: CORVET and HOPS. FEBS J 280, 2743–2757.
Sriram V, Krishnan KS, Mayor S (2003). deep-orange and carnation define distinct stages in late endosomal biogenesis in Drosophila melanogaster. J Cell Biol 161, 593–607.
Starai VJV, Hickey CMC, Wickner WW (2008). HOPS proofreads the trans-SNARE complex for yeast vacuole fusion. Mol Biol Cell 19, 2500–2508.
Steinman RM, Mellman IS, Muller WA, Cohn ZA (1983). Endocytosis and the recycling of plasma membrane. J Cell Biol 96, 1–27.
Stroupe C, Collins KM, Fratti RA, Wickner W (2006). Purification of active HOPS complex reveals its affinities for phosphoinositides and the SNARE Vam7p. EMBO J 25, 1579–1589.
Swetha MG, Sriram V, Krishnan KS, Oorschot VMJ, Brink ten C, Klumperman J, Mayor S (2011). Lysosomal membrane protein composition, acidic pH and sterol content are regulated via a light-dependent pathway in metazoan cells. Traffic 12, 1037–1055.
Tornieri K, Zlatic SA, Mullin AP, Werner E, Harrison R, L'hernault SW, Faundez V (2013). Vps33b pathogenic mutations preferentially affect VIPAS39/SPE-39-positive endosomes. Hum Mol Genet 22, 5215–5228.
Treusch S, Knuth S, Slaugenhaupt SA, Goldin E, Grant BD, Fares H (2004). Caenorhabditis elegans functional orthologue of human protein h-mucolipin-1 is required for lysosome biogenesis. Proc Natl Acad Sci USA 101, 4483–4488.
Wang C-W, Stromhaug PE, Kauffman EJ, Weisman LS, Klionsky DJ (2003). Yeast homotypic vacuole fusion requires the Ccz1-Mon1 complex during the tethering/docking stage. J Cell Biol 163, 973–985.
Wickner W (2010). Membrane fusion: five lipids, four SNAREs, three chaperones, two nucleotides, and a Rab, all dancing in a ring on yeast vacuoles. Annu Rev Cell Dev Biol 26, 115–136.
Xiao H, Chen D, Fang Z, Xu J, Sun X, Song S, Liu J, Yang C (2009). Lysosome biogenesis mediated by vps-18 affects apoptotic cell degradation in Caenorhabditis elegans. Mol Biol Cell 20, 21–32.
Xu L, Sowa ME, Chen J, Li X, Gygi SP, Harper JW (2008). An FTS/Hook/p107(FHIP) complex interacts with and promotes endosomal clustering by the homotypic vacuolar protein sorting complex. Mol Biol Cell 19, 5059–5071.
Zick M, Wickner W (2013). The tethering complex HOPS catalyzes assembly of the soluble SNARE Vam7 into fusogenic trans-SNARE complexes. Mol Biol Cell 24, 3746–3753.